

# Chapter 4

---

*Landslide Analysis and Interpretation*

## 4 Landslide Analysis and Interpretation

### 4.1 Hydrological Interpretation

Landslide is a phenomenon by which some or all of a slope mass slowly moves down the slope under the influence of groundwater and gravity. Therefore, the most important mechanism that triggers landslides is fluctuation of groundwater level. Generally, changes to groundwater level are due to rainfall. The rainfall amount related to groundwater has been monitored using two rain gauges since August 2010, and the groundwater level has been monitored six water level gauges installed in 2010 and five water level gauge in 2011. Unfortunately the data logger from one of the water gauges was stolen, so only ten sets are still operating.

#### 4.1.1 Characteristics of rainfall

The record of the rain gauges installed in the Abay Gorge area could be described as follows.

- The mean annual rainfall is relatively low at about 1,200-1,400mm.
- It rains intensively, 600-700mm, for two months, July and August of the rainy season, when about 50% of annual rainfall is recorded.
- It rains at least once a day on most days in July and August. Monthly rainfall exceeds 300mm and the average for July is about 10mm per day.

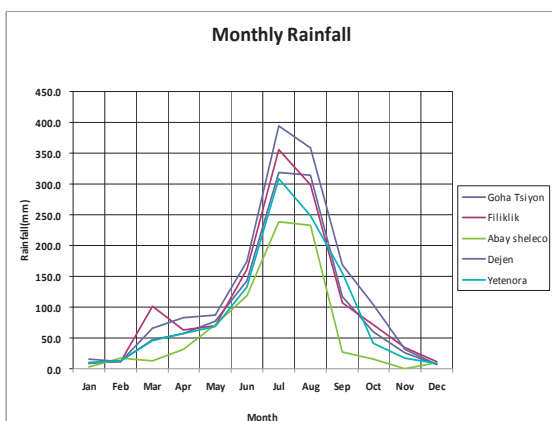


Figure 4.1.1 Mean monthly rainfall (Unit: mm/month)

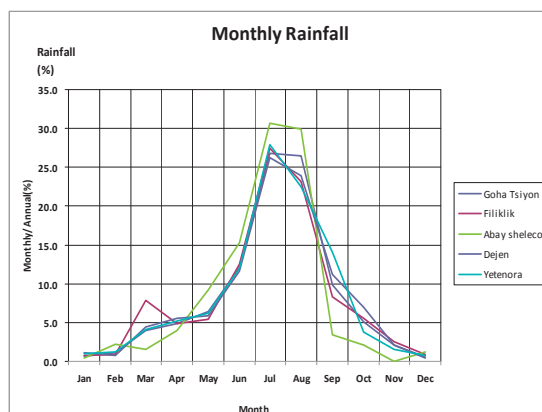


Figure 4.1.2 Mean monthly rainfall (Unit: %/year)

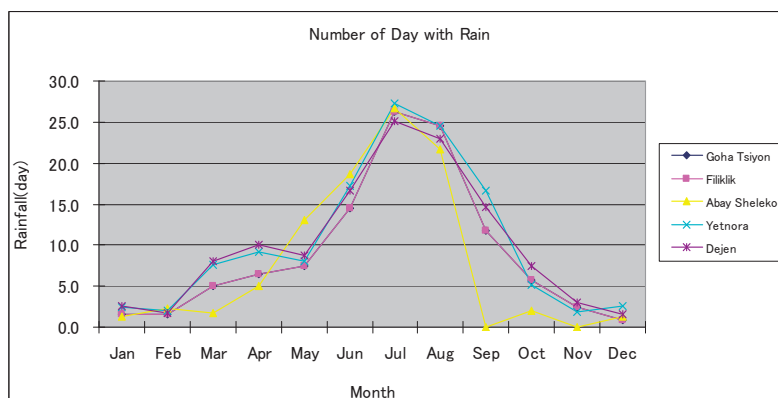


Figure 4.1.3 Mean monthly number of days with rain

#### 4.1.2 Landslide occurrence and triggering mechanisms

Table 4.1.1 displays the records of landslide occurrences in the Abay Gorge in recent years.

Table 4.1.1 Landslide Occurrence

Station No.	Time	Observed damage
ST.0+700- ST.1+100	2008 rainy season	Road settlements Every rainy season
	2009 rainy season	ditto
	2010 rainy season	ditto
ST.4+900- ST.5+200	2006 Aug~Sep	Collapse of existing retaining wall
ST.21+850- ST.22+200	2008 rainy season	Collapse of retaining wall
	2009 rainy season	Landslide area expansion
ST.27+500- ST.27+800	2006 unknown	Old church destroyed New church under construction (cracks found)
	Every rainy season	Road subsidence
	ST.28+100- ST.28+600	Every rainy season
ST.32+250	2009	Road culvert is damaged

JICA (2010)

These records indicate that the landslides are occurred mainly in the rainy season of July-September.

There are many mechanisms that cause landslides, such as geomorphological features, geology, and other man-made and natural conditions. In the Abay Gorge, water is the direct and primary cause of a landslide. Since groundwater is fundamentally recharged by rain, the relation between a landslide and rain is close. According to Takano, 1960, landslides occur most easily when about 10 mm/day of rainfall continues for about five days. This is because rainfall of this level is most suitable for deep percolation. Otherwise rainfall heavier than this seldom permeates into the ground and becomes a surface flow.

Theoretically, when groundwater increases the pore water pressure also increased, and effective stress will decrease. As a result, shear resistance decreases and triggered a landslide.

The following figure is an example of landslide measurement (Takano, 1960). The groundwater level and the amount of movement correlate splendidly.

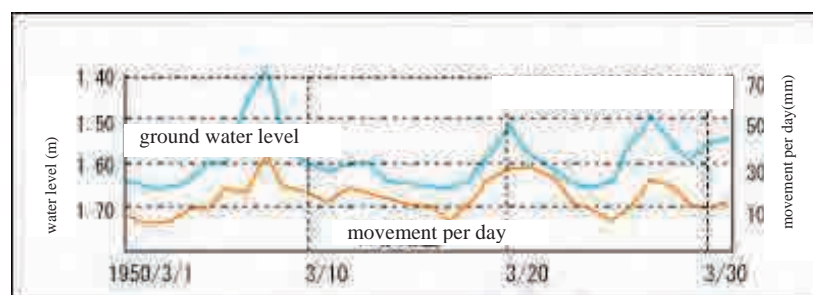


Figure 4.1.4 Example of landslide measurement vs. Groundwater level

Note: Correlation between groundwater level (blue) and movement (orange) of a chronic landslide. The left Y-axis represents groundwater level (m) and the right,

daily movement (mm) of the landslide; while the X-axis is the date  
(year/month/day).

### 4.1.3 Hydrological monitoring data interpretation

The locations of monitoring stations and specifications of the pressure type water gauges that are installed in the drilling holes since August, 2010 are shown in Table 4.1.2.

Table 4.1.2 Monitoring sites and parameters

No.	Location	Site	Drilling survey		Groundwater level meter	Monitoring started
			No.	Core drilling		
1	ST.0+800 - ST.1+100	L/S00	B00-14	30m	30m	21 Jul. 2011
			B00-21	30m	30m	3 Aug. 2010
2	ST.4+800 - ST.5+500	L/S05	B05-12	30m	30m	14 Aug. 2010
			B05-13	35m	35m	7 Jul. 2011
			B05-31	35m	35m	1 Sep. 2010
3	ST.27+500 - ST.27+900	L/S27	B27-09	50m	50m	29 Jun. 2011
			B27-10	25m	25m	15 Jun. 2011
			B27-11	25m	25m	24 Sep. 2010
			B27-23	25m	25m Data logger stolen(Nov.)	8 Oct. 2010 * stolen
4	ST.28+000 - ST.28+700	L/S28	B28-21	25m	25m Data logger stolen(Nov.)	9 Sep. 2010 * stolen
			B28-23	30m	30m	15 Jun. 2011

Two of the six data loggers, B27-23 and B28-21, were stolen after data was acquired on November 25, and since then there has been no measurement record. Monitoring is still being carried out at the other gauges, and the rainfall records of each station are summarized as graphs in Appendix.

At water level meter B00-14, the steady water level keeps about -23 to -24m after July 2011. At water level meter B00-21, the steady water level of -20 to -23m and the high water level of -18.1m from August 2010 to September 2010 were recorded. The steady water level keeps about -20m after October 2010. Continued monitoring is required for confirmation.

At water level meter B05-12, the steady water level -31 to -32m and the high water level -31.0m at August 15 was recorded. However, the data has not been recorded since October 9 because there has been no water in the hole. At water level meter B05-13, the data has not been recorded since the installation because there has been no water in the hole. At water level meter B05-31, the steady water level of -22 to -23m and the high water level of -21.8m on September 2011 were recorded.

At water level meter B27-09, the steady water level of -15 to -16m had been recorded. However, the monitoring has never been implemented since July 26, 2011 because of the landslide movement. At water level meter B27-10, the steady water level of -21 to -23m and the low water level of less than -25m at the end of July 2011 were recorded. At water level meter B27-21, the steady water level of -22 to -23m and the high water level of -21.9m on September 29 in the rainy season were recorded. The steady water level keeps about -23 to -24m in the dry season. At water level meter B27-23, the steady water level of -20 to -21m and the high water level of -20.3m on November 8 were recorded. However, there is no data after November 24 because the equipment was stolen.

At water level meter B28-21, both the steady water level and the high water level keeps around -20m. However, there is no data after November 24 because the equipment was stolen. At water level meter B28-23, the rising up according to the rain and the high water level at -14.7m observed. The steady water level of -15 to -17m has been recorded after that.

Dalliance of installation of devices couldn't allow making full monitoring of water level changes during the rainy season (around July to September). However, future monitoring could reveal the relevance of rainfall to groundwater level variation.

## 4.2 Hydrographic System

The Abay River divides the Project area into north and south sections, and is located upstream of the Blue Nile River. Moreover, the Blue Nile River originates from Lake Tana, which is about 150km (direct distance) north of the Project area. Abay bridge is about 285km from Lake Tana, and the gorge section is roughly, about 1,500m from top to bottom.

The river channel altitude around the Abay Bridge is about 1,000m, and its width is about 200m. All the areas for investigation are in the drainage basin of Abay River. Even though the amount of water of Abay River decreases in the dry season, it does not dry up totally. However, some of its tributaries entirely lose water by the end of the dry season. Moreover, ponds that form in the rainy season also disappear at the end of the dry season.

### 4.2.1 Drainage network

The river network of the section between Dejen and Goha Tsiyon applicable to this investigation is shown in Figure 4.2.1, and was created using the data below. After overlaying all data in a GIS and checking their spatial relationship, and also considering the results of the field survey, the final river network figure was compiled. The river names used are adopted from the topographic maps prepared by the Ethiopia Mapping Agency.

When this river network figure is considered the mechanisms of landslide (i.e., the relation between landslide and water) become apparent. Moreover, this data will be very important in future when taking into consideration the drainage works in landslide countermeasures.

- 1) Topographical maps produced by the Project  
Scale: 1/5,000  
Date of production: July 2010
- 2) Satellite (ASTER) data  
Contraction (Flat plane graphic mode): 30m  
Date of capture: After 2000
- 3) Topographical maps by the Ethiopia Mapping Agency  
Scale: 1/50,000  
Published: 1984

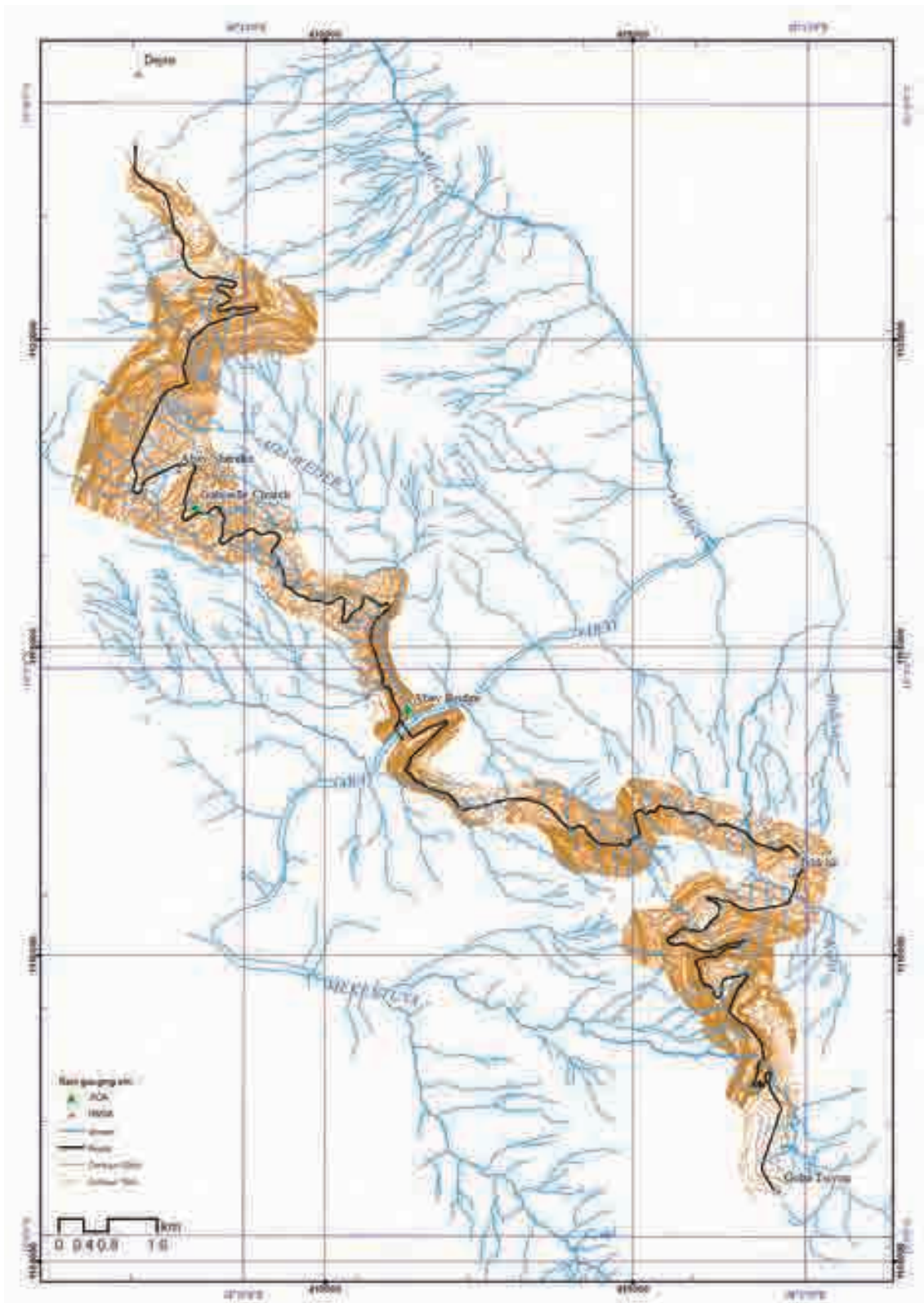


Figure 4.2.1 Drainage network



#### 4.2.2 Groundwater distribution and flow

Although five landslides were considered in the current investigation only eleven water level monitoring stations have been installed, meaning there is no conclusive data on the rainy season. Therefore, the relevance of rain and groundwater level can not be fully confirmed. However, if the geographical feature and the valley in the target landslide area are taken into consideration, it is clear that the water which flowed into the osmosis and the mountain streams of surface water by rain turned into groundwater, and has contributed to the rise of the groundwater level.

In addition, further water gauges are due to be added from now on. Therefore, it seems by grasping change of another amount of spring water the change of the groundwater level, the situation of spring water, the groundwater distribution and the flow situation becomes clear.

The points where spring water is currently being checked in the field survey are shown in Figure 4.2.2 to Figure 4.2.4

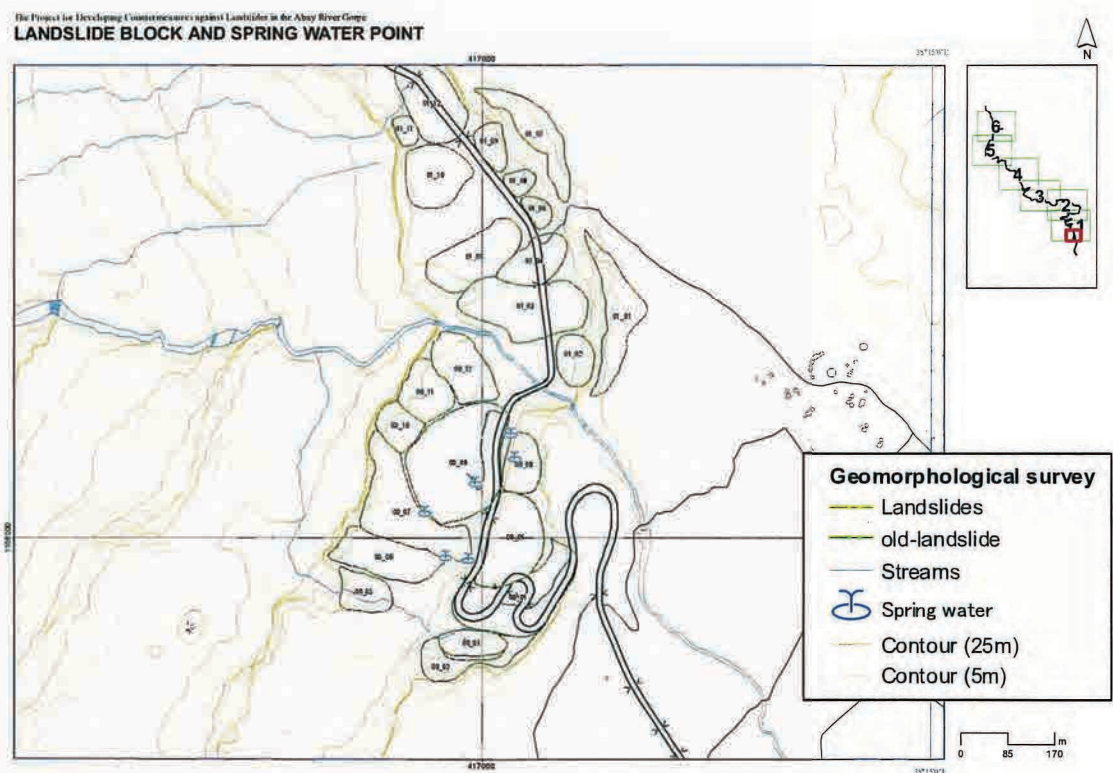


Figure 4.2.2 Landslide Block and Spring Water Point (L/S00)

The Project for Developing Countermeasures against Landslides in the Abay River Gorge  
**LANDSLIDE BLOCK AND SPRING WATER POINT**

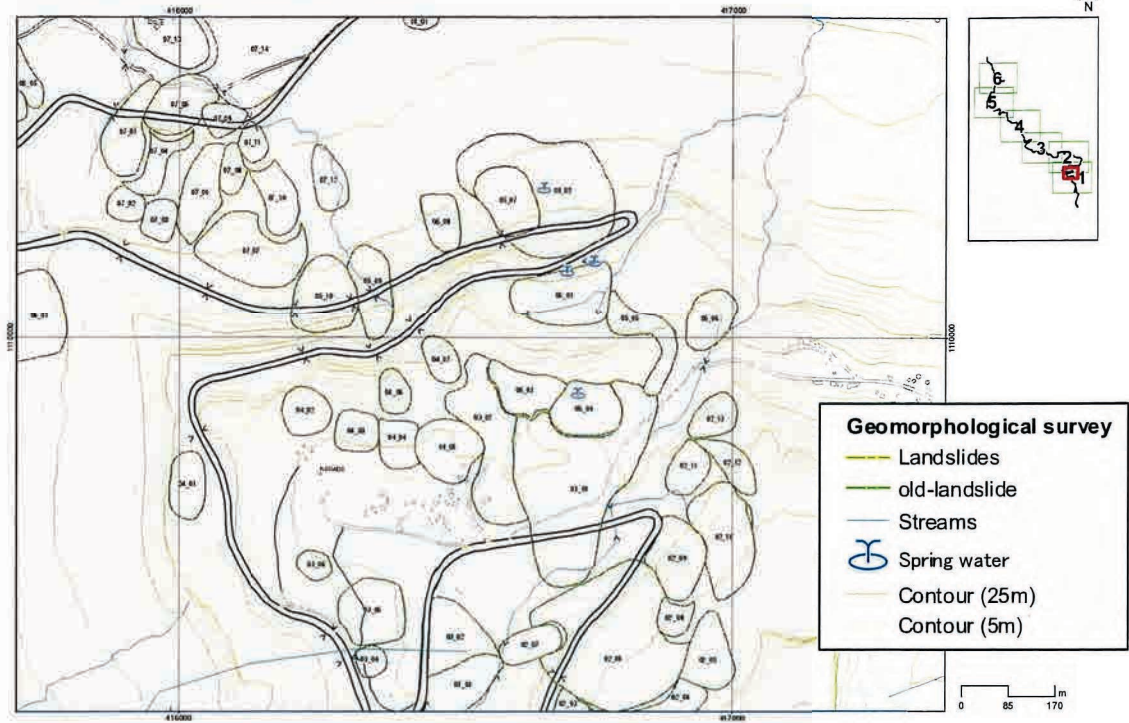


Figure 4.2.3 Landslide Block and Spring Water Point (L/S05)

The Project for Developing Countermeasures against Landslides in the Abay River Gorge  
**LANDSLIDE BLOCK AND SPRING WATER POINT**

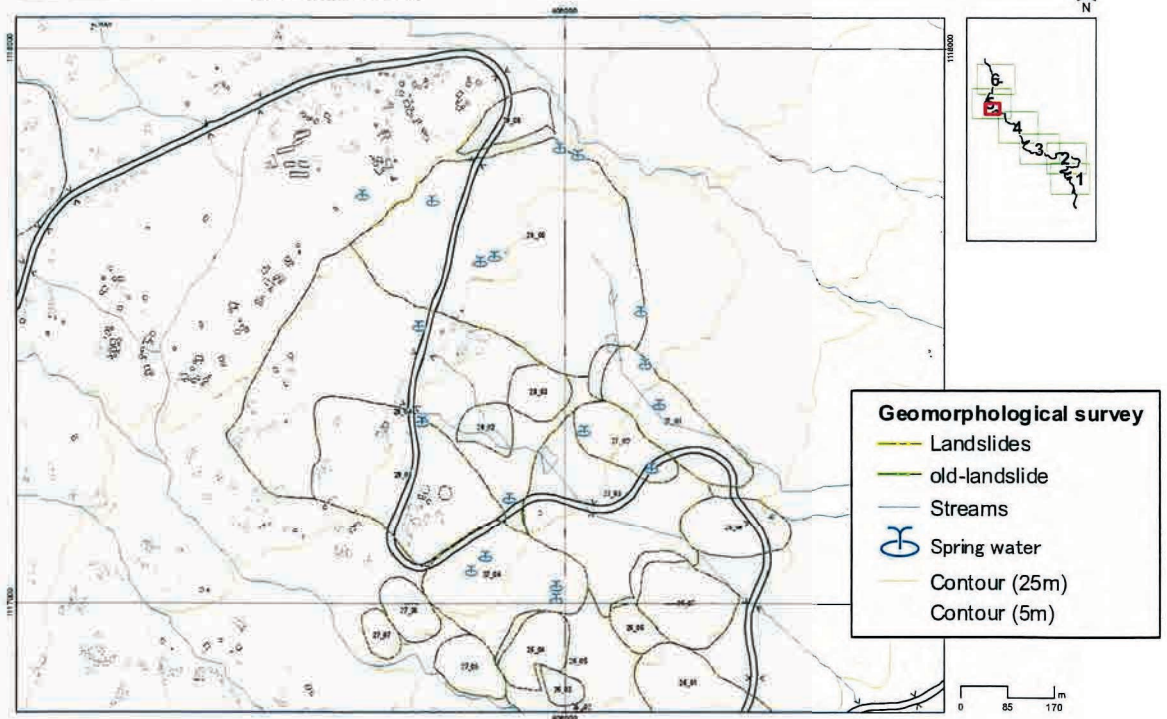


Figure 4.2.4 Landslide block and spring water point (L/S27 and 28)



## 4.3 Landslide area Identification and Assessment

### 4.3.1 Satellite imagery interpretation

There are many large landslides, which probably are produced during the formation of the Abay Gorge. These old landslides can be clearly identified from satellite images.



Figure 4.3.1 Examples of old landslides (L/S05-01)

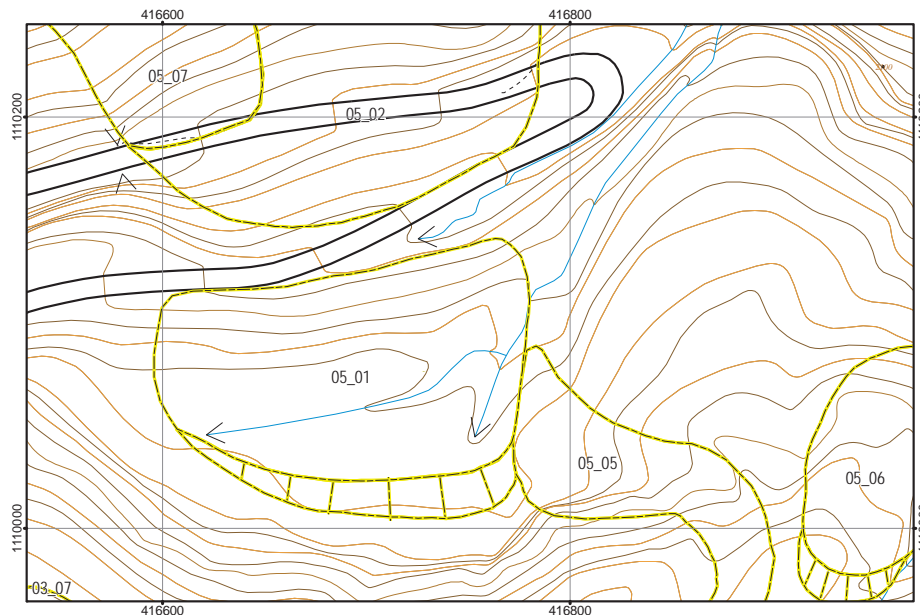


Figure 4.3.2 Interpreted landslide map around station (L/S05-01)

Figure 4.3.1 shows the result of satellite imagery interpretation near L/S05-01. The horseshoe-shaped steep cliff surrounding the landslide block at L/S05-01 is the main scarp of the old huge landslide that formed this horseshoe-shaped cliff in ancient times. Thereafter, moving mass by a landslide that occurred on the upper part (L/S03-01, etc.) was piled up at the head of the lower landslide, and then a secondary landslide occurred. The secondary landslide can be interpreted as being at L/S05-01.

Figure 4.3.2 shows map of landslides from the satellite imagery interpretation around the landslide block at L/S05-01. Here, the main scarp of the old landslide is not interpreted as a main scarp of the current landslide; a main scarp in the Project is defined as a head crown of a landslide which is moving at the moment.

As a similar example, Figure 4.3.3 shows the result of satellite imagery interpretation near L/S07-11. The round hill at the center of the figure represents an old landslide. The steep cliff behind it, on the southern side of the road (lower-right portion of the photo), can be interpreted as the old main scarp. Figure 4.3.4 shows map of landslides from the satellite imagery interpretation. The moved portion of the old landslide is interpreted as a landslide block. However, the main scarp of the old landslide is not interpreted as a main scarp of a current landslide.

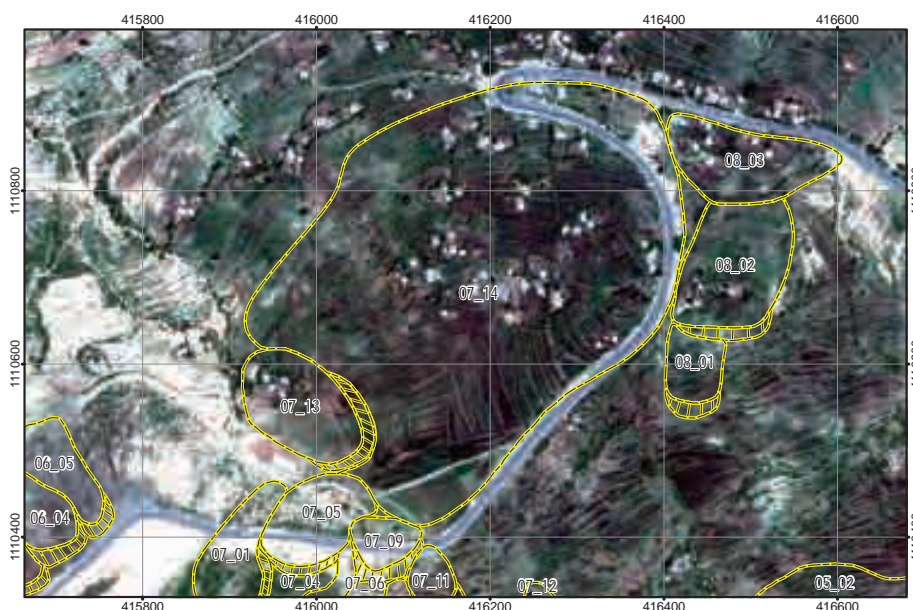


Figure 4.3.3 Examples of old landslide (L/S07-14)

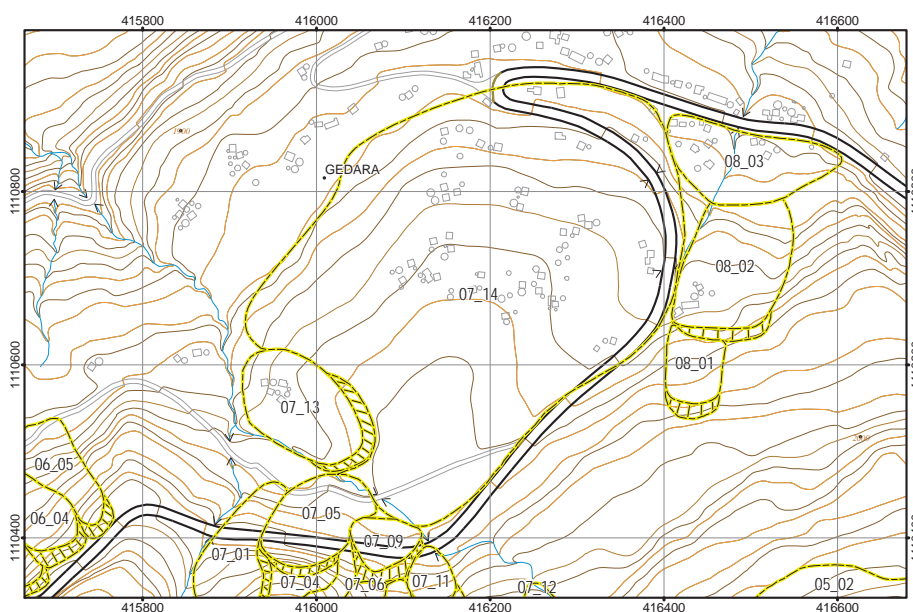


Figure 4.3.4 Interpreted landslide map around station (L/S07-14)



The area from L/S26 to L/S28 has a widely distributed colluvial deposit and contains multiple landslides, these are distributed in multiple layers, so it is difficult to identify and extract single landslides.

Among the landslide topographies that can be identified from satellite imagery, (1) the range where a landslide can be clearly identified and (2) the range where a moving block can be identified as an event on the ground surface, such as deformation of a road or formation of a new main scarp, are interpreted as a landslide block. Global Positioning System (hereafter GPS) measurements were used when the boundary between two landslide blocks was not clear only from interpretation of satellite imagery. The boundary between the blocks was determined using the road deformation and the crack distributions by GPS measurements. The landslides identified in this area are showed in Figure 4.3.6.

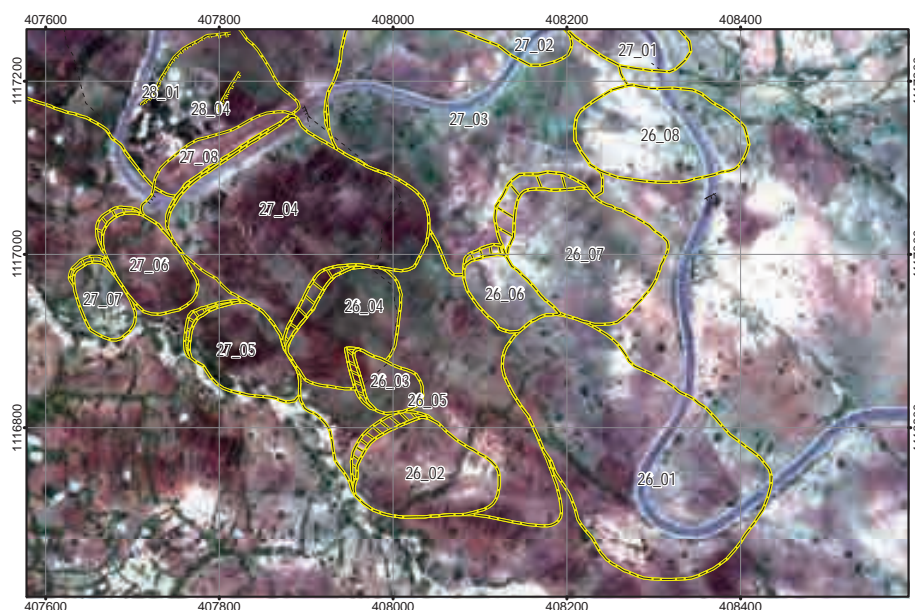


Figure 4.3.5 Satellite imagery interpretation and mapping of landslides (L/S26 to L/S27)

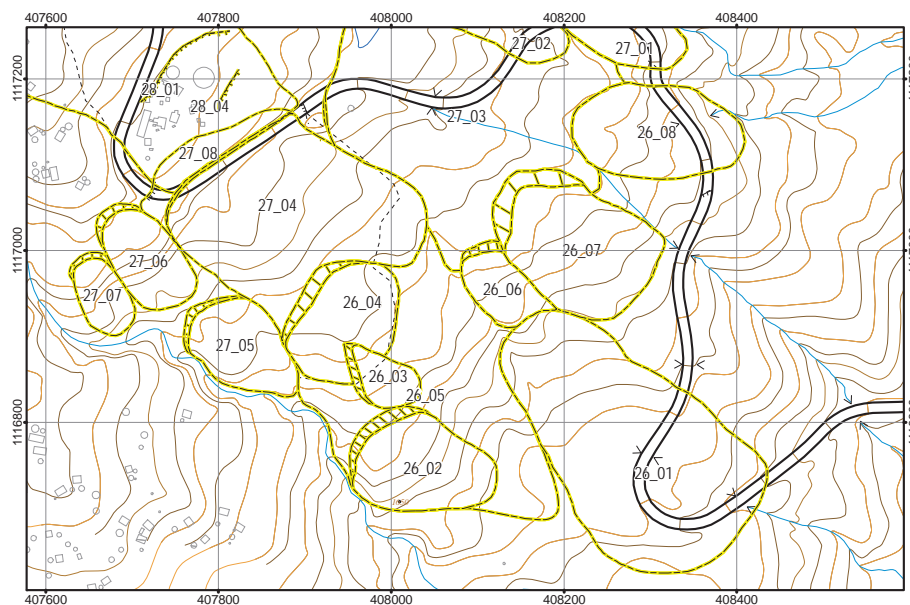


Figure 4.3.6 Interpreted landslide map around station (L/S26 to L/S27)

### 4.3.2 Landslide distribution

Landslides which are shown in the landslide distribution map are classified into blocks, according to the movement direction, scale, activity and mechanism.

A landslide distribution map is created after identifying the landslide landform from satellite photos and conducting a field survey to grasp and classify the conditions of the main scarps, cracks, steps and moving mass and confirm the detailed landslide boundary. To create this map, the landslide distribution and changes over the last 30 years were identified by reading the Geo-Eye 1 satellite photos (taken on June 3 and 7, 2010) and the aerial photos taken by the EMA in 1982. The results obtained by interpreting the photos were confirmed at the site to determine if any modifications and/or additions were needed.

The results of aerial and satellite image interpretations were combined with those of the rockfalls and debris flow analysis. They were compiled into the “landslide, rockfall and debris flow hazard map” organized using GIS. The “landslide distribution map” will be finalized by incorporating the results of not only the topographical survey but also the study of the landslide history, geological survey and two-year monitoring.

The relationship between the landslides, altitude and basement geology was analyzed to study the distribution and trend of the landslides in the surveyed area.

#### a. Number of landslides by altitude

The data on landslide distribution and altitude were combined using GIS to study the relationship between the number of landslides and the altitude. With respect to the number of landslides for every 200m altitude, on the Goha Tsiyon side, the number is highest between 2,400 and 2,600 m, followed by 2,000 and 2,200 m, and 2,200 and 2,400 m. On the Dejen side, many landslides are observed between 1,800 and 2,000 m, while few are observed at other altitudes.

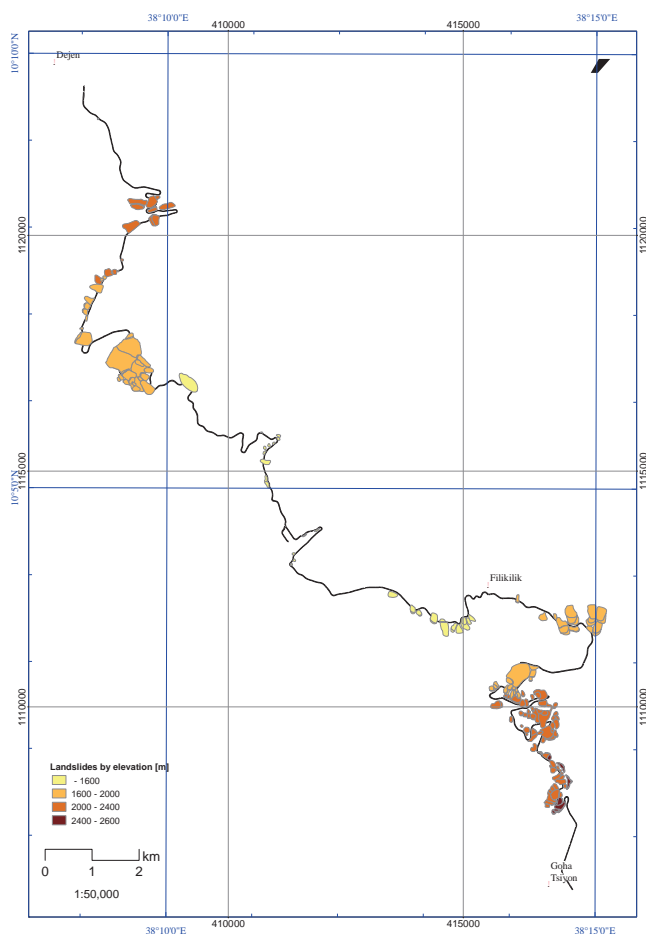


Figure 4.3.7 Mapping of Landslide Distribution by Altitude

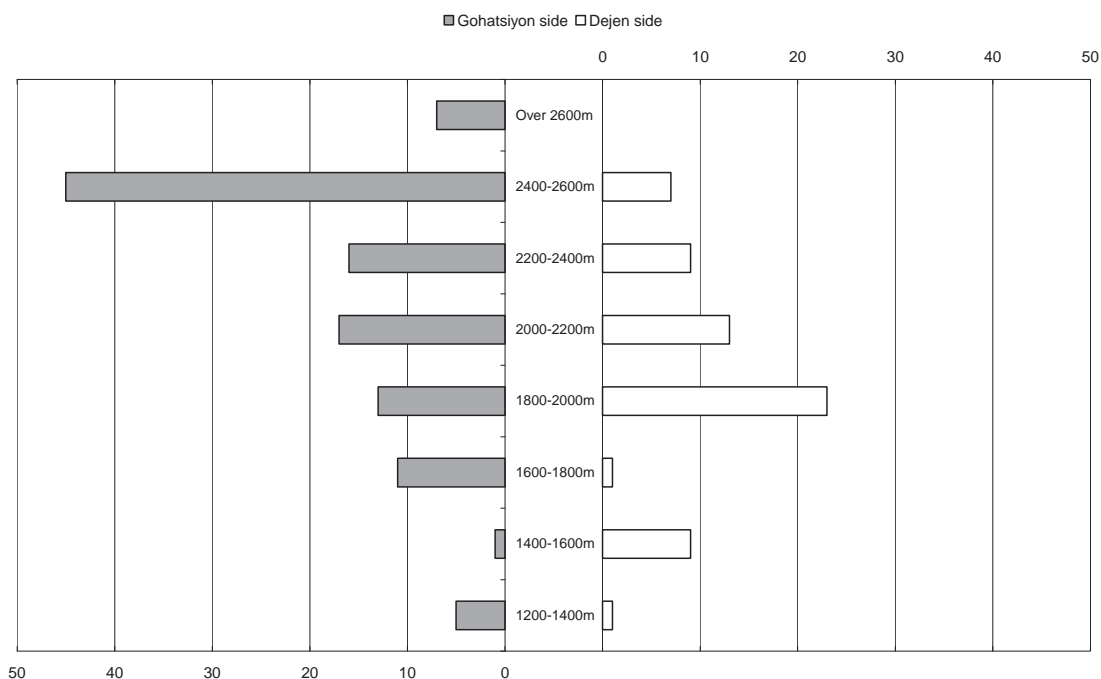


Figure 4.3.8 Landslide Distribution by Altitude (Left: Goha Tsiyon side, Right: Dejen side)

### b. Number of landslides by geology

In general, colluvial deposits are accumulated essentially under scarps and on gentle slopes. The data on landslide distribution and geology of the bedrock were combined by GIS to study the relationship between the number of landslides and the bedrock geology. In terms of the number of landslides per km<sup>2</sup> area, the landslide frequency is the highest (17.45 per km<sup>2</sup>) in the area of limestone, siltstone and shale of the Antalo Formation, followed by area covered with basalt and pyroclastic rock (12.62 per km<sup>2</sup>). The frequency is low in the area with gypsum, siltstone and shale in the Abay Formation and the area with sandstone and conglomerate in the Adigrat Formation. Both formations are located at low altitudes in Abay Gorge.

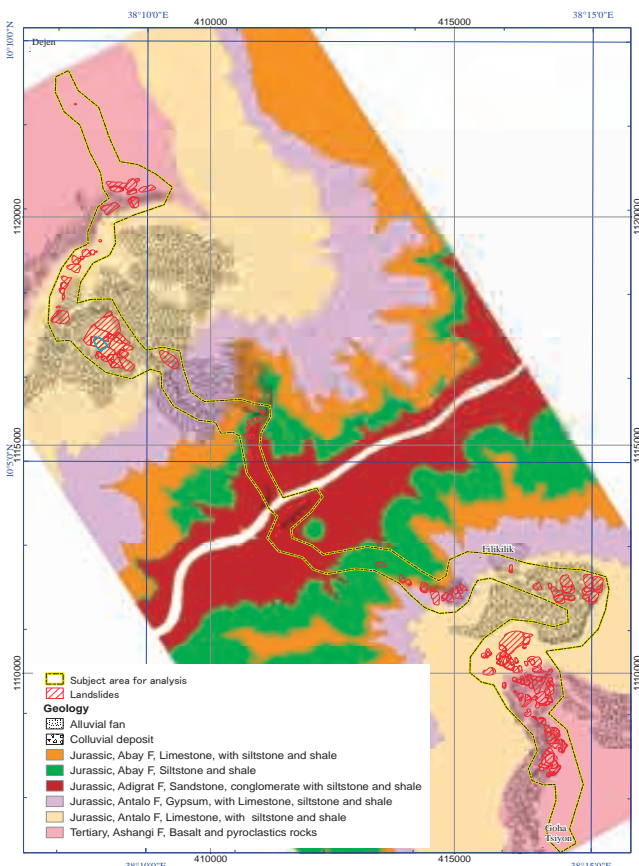


Figure 4.3.9 Geological Map with Landslide Overlay

Table 4.3.1 Landslide Density by Geology

<b>Geology</b>	<b>Road length by geology [m]</b>	<b>Area of each geology [km<sup>2</sup>]</b>	<b>Number of landslides [Landslides]</b>	<b>Density in each geology [Landslides/km<sup>2</sup>]</b>
Basalt and pyroclastic rocks	20659.56	5.39	69	12.81
Limestone, with siltstone and shale	9181.99	8.59	82	9.54
Gypsum, with Limestone, siltstone and shale	3827.89	1.74	7	4.03
Siltstone and shale	2023.25	1.08	3	2.77
Sandstone, conglomerate with siltstone and shale	5386.58	1.76	12	6.83

(Colluvial deposits have been excluded because some colluvial deposits are themselves landslide mass)



### 4.3.3 Characteristics of landslide blocks

The micro landforms of landslides are summarized in Figure 4.3.10. Landslides with significant movement clearly show in the landforms. The main scarp (or horse shoe shape scarp) is one such landform where landslides are most easily recognizable. Depression zones, tension cracks, ponds and swamps are observed at upper part on the landslide. Located middle to upper part on the landslide is small isolated hummocks. The bottom of the landslide protrudes from the surrounding slope and compression landforms such as compression cracks, pressure ridges and pressure wrinkles are observed. The tongue is pushed out forward and downward and it sometimes changes the course of a river.

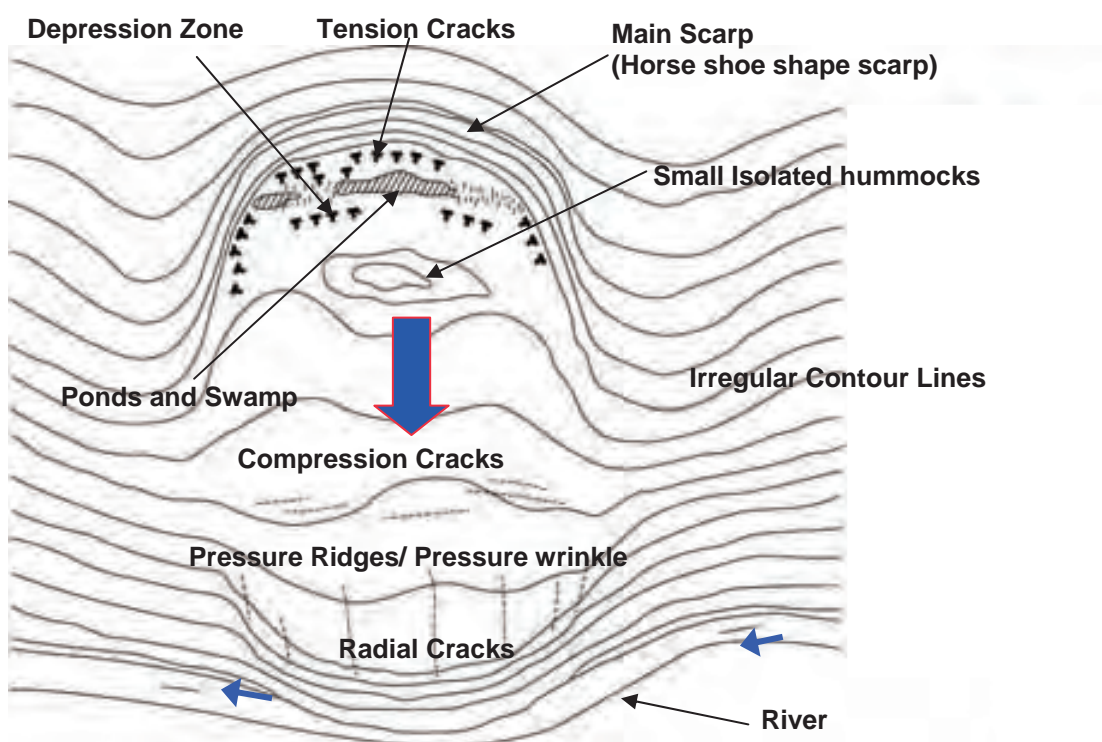


Figure 4.3.10 Schematic Diagram of Landslide Landforms

Photo 4.3.1 shows a depression zone commonly found at the upper part of a landslide. There are two or more parallel normal steps confronting each other and a belt-shaped low-lying area is often observed. There is a depression zone at point ST.28. There are multiple depressions on the mountain side and the area between the steps and the main scarp is the depression zone. The high-lying area consists of an isolated hummock.



Photo 4.3.1 Depression Zone at Upper part of Landslide

A pond is sometimes observed in the depression zone at the upper part of a landslide. Photo 4.3.2 shows the pond that appeared in a field near Kurar Village. Due to the ridges caused by the landslide, the bottom of the landslide was uplifted. As a result, a relatively depressed area was formed where water gathered. Nearly 10 ponds and ground depressions with traces of water build-up are observed scattered around this area.



Photo 4.3.2 Pond that Appeared in Field near Kurar Village

Steps are often observed in landslide areas (Photo 4.3.3). In areas where there is a step crossing the road, the road surface is often deformed, hampering the movement of vehicles. Also, the fields in Abay Gorge have artificial steps and stone fences, which are mostly difficult to distinguish from steps caused by landslides.



Photo 4.3.3 Step Caused by Landslide

Landforms at the end of a landslide include pressure ridges and pressure wrinkles caused by the compression force of the landslide. The soil mass at the rear has been uplifted onto the land (Photo 4.3.4). Also, the end of the landslide tends to be unstable and collapse is liable to occur on steep slopes consisting of landslide mass. Collapse is liable to occur at the end of an active landslide as well as at the end of a steep landslide.



Photo 4.3.4 Ridge Caused by Compression Force of Landslide

When interpreting topographic maps, it is possible to deduce the existence of landslides from the irregular contour lines. Figure 4.3.11 is a topographic map of the vicinity of Kurar Village on the Dejen side. The area to the left is not a landslide area. The contour lines are parallel and drawn in an orderly manner. The rivers flow relatively straight. On the other hand, the area to the right is a landslide area. The contour lines are irregular and the river courses are often interrupted. Since surface water easily permeates through cracks in a landslide area, the water spreads underground, making it difficult for rivers to form.

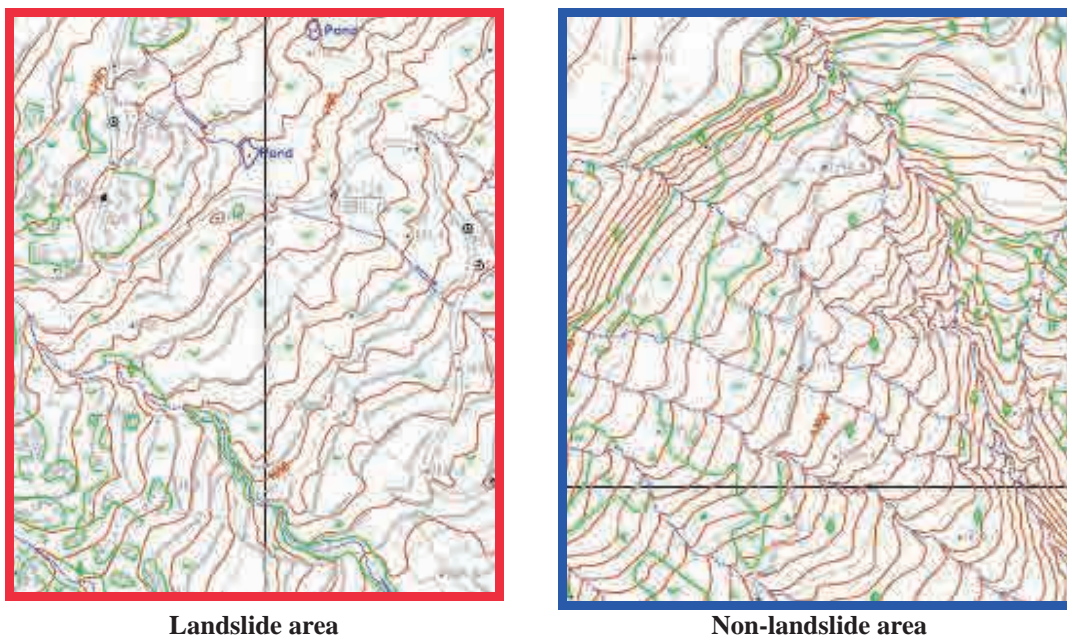


Figure 4.3.11 Comparison of Contour Lines in Landslide Area and Non-landslide Area



#### 4.3.4 Landslide hazard assessment

The results of the landslide hazard assessment, combined with those of rockfall and debris flow hazard assessment, will constitute a comprehensive “sediment disaster hazard map”.

With respect to the assessment method, the score rating system commonly used in Japan is adopted, but the score rating of the system has been confirmed to make it suitable for the evaluation results by the experts, incorporating the characteristics of the landslides in the Abay Gorge area.

The sediment disaster hazard map is created using GIS to make it as easy to understand as possible so that it can serve as a basic reference when studying the priority of countermeasures and the road management in the future.

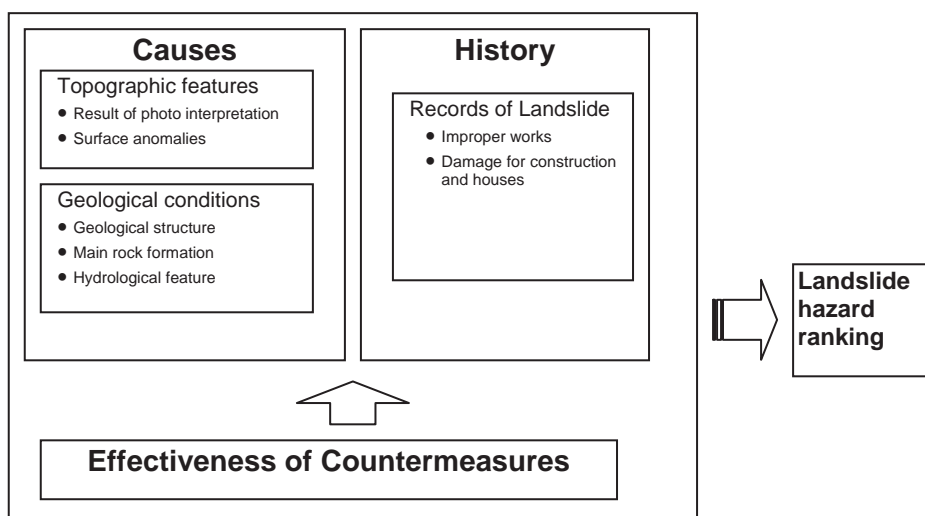


Figure 4.3.12 Flowchart of Landslide Hazard Assessment

Table 4.3.2 Landslide Hazard Assessment Categories and Scores

Category		4	2	1	0	
<b>A: Causes</b>	Topographical factor	Result of photo interpretation	exist clearly	exist but partial and not clear	exist but not clear	
		Surface anomalies	large and new cracks, steps and subsidence	small and old cracks, steps and subsidence	slight deformation	no anomalies
	Geological conditions	Geological structure		step, fracture / dip slope	undip slope and others)	
		Main rock formation of landslide body	pyroclastic materials(Py)	colluvial deposit(Co) / siltstone(Si)	basalt(Ba) / shale(Sh) / limestone(Lm)	sandstone(Ss) / gypsum(Gy)
		Hydrological feature	much springs / seepage	little springs / little seepage	surface water / trace of water	no water observed
<b>B: History</b>	Records of Landslide	Improper works		obvious	slight	not exist
		Damage on construction and houses	obvious	slight		no indication/ no constructions)
<b>C: Effectiveness of Countermeasure</b>		No countermeasure: ± 0	No effect: ± 0	Some effect: -2	High effect: -4	

In addition, the landslide risk for the road was assessed in qualitative terms, taking into consideration the landslide hazard and the impact on the road. The impact on the road was determined based on the positional relationship between the landslide and the road and whether or not the landslide phenomenon affects the road. The higher the landslide hazard rank and the greater the impact on the road, the higher the landslide risk for the road.

Table 4.3.3 Landslide Risk Assessment of the Road

		Influence on the road			
		A	B	C	D
Landslide hazard	A	I	II	III	IV
	B	II	III	IV	IV
	C	III	IV	IV	IV

Table 4.3.4 and Table 4.3.5 are summary of the procedures of risk assessment for each landslide. The each result of risk assessment for a total of 167 landslide blocks is shown in Appendix

A summary of the risk assessment results is provided in Appendix.

Figure 4.3.13 is a graph showing the relationship between the landslide hazard rank and the number of landslide blocks. Of the 167 landslide locations, 23% are ranked A (highest risk).

Figure 4.3.14 is a graph showing the relationship between the risk level considering the influence on roads and the number of landslide blocks. 13% of the blocks are ranked I (highest risk), while 24% are ranked II.

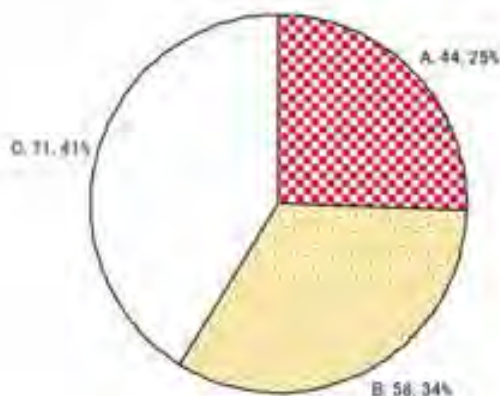


Figure 4.3.13 Landslide Hazard Rank and the Number of Landslide Blocks

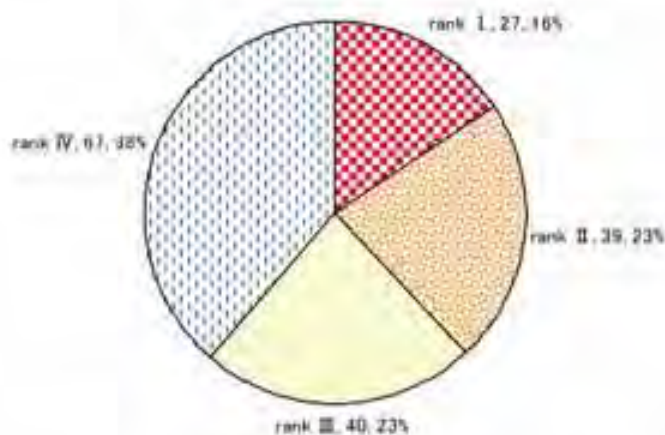


Figure 4.3.14 Rank of Risk on Roads and the Number of Landslide Blocks

#### 4.3.5 Priority landslides

According to the results of landslide risk assessment of roads (chapter 4.3.4), landslides of rank I (extremely high risk to the road) and rank II (high risk to the road) should be regarded as high priority landslides. ERA has already carried out construction work as a countermeasure for some sections of the high priority landslide. Drilling survey, monitoring and geophysical exploration have been conducted in several sections of the high priority landslide as part of the Project. The high priority landslides are as follows:

Table 4.3.4 High Priority Landslides on Goha Tsiyon side

Landslide No.	Location [km]	Influence to the road A: Serious/On the road B: Slightly serious/ Near the road C: Slight influence D: No influence	Hazard Rank by the Score A: High hazard B: Middle hazard C: Relatively low hazard	Risk for the Road =Hazard X D	Remarks
				I : Extremely High Risk II : High Risk III: Middle Risk IV: Relatively Low Risk	
00-04	0.7-0.8	A	B	II	
00-07	0.7-0.8	B	A	II	
00-08	0.9-1.1	A	A	I	monitoring site
00-09	0.9-1.0	A	A	I	cut slope, topple, monitoring site
00-12	1.0-1.1	B	A	II	artificial fills
01-06	1.3-1.4	A	B	II	collapse
01-08	1.4-1.5	A	B	II	
01-09	1.5-1.6	A	A	I	
01-12	1.6-1.8	A	B	II	
01-14	1.9-2.0	A	B	II	
02-01	2.0-2.0	A	B	II	
02-03	2.3-2.4	A	A	I	
02-06	2.5-2.7	A	A	I	
02-09	2.7-2.8	A	A	I	bad ditch, collapse
03-01	3.0-3.2	A	B	II	'Countermeasures was completed
05-01	4.9-5.02	A	A	I	monitoring site
05-02	5.05-5.1	A	A	I	monitoring site
05-03	4.9-5.02	B	A	II	
05-04	4.9-5.02	B	A	II	
05-05	5.1-5.1	B	A	II	
05-07	5.4-5.6	A	A	I	
05-08	5.6-5.7	A	B	II	
05-10	5.8-5.93	A	B	II	collapse
07-05	7.0-7.1	A	B	II	collapse
07-09	7.1-7.2	A	B	II	
10-04	10.4-10.5	B	A	II	
10-05	10.5-10.7	A	A	I	
10-06	10.7-10.8	A	A	I	
13-07	13.8-14.0	A	B	II	
13-08	13.9-14.0	A	B	II	
14-01	14.2-14.4	A	B	II	gypsum quarry

Table 4.3.5 High Priority Landslide on Dejen side

Landslide No.	Location [km]	Influence to the road	Hazard Rank by the Score	Risk for the Road =Hazard X D	Remarks
		A: Serious/On the road B: Slightly serious/ Near the road C: Slight influence D: No influence	A: High hazard B: Middle hazard C: Relatively low hazard	I : Extremely High Risk II : High Risk III: Middle Risk IV: Relatively Low Risk	
20-01	20.1-20.3	A	B	II	collapse on cut slope
21-01	20.9-21.1	A	B	II	collapse on cut slope
21-02	21.2-21.4	A	B	II	cut slope
21-03	21.5--21.7	A	B	II	
21-06	21.8-21.8	B	A	II	cut slope
22-01	21.9-22.0	B	A	II	monitoring site
25-01	25.2-25.7	A	B	II	
26-01	26.33-26.7	A	B	II	
26-08	26.8-27.0	A	A	I	
27-01	27.02-27.2	A	A	I	
27-02	27.2-27.3	A	B	II	
27-03	27.2-27.6	A	B	II	
27-04	27.6-27.7	A	A	I	
27-06	27.8-27.82	B	A	II	
27-08	27.0-27.2	A	A	I	
28-01	27.9-28.1	A	A	I	monitoring site
28-04	28.1-28.3	A	A	I	monitoring site
28-05	28.3-28.6	A	A	I	monitoring site
28-06	28.6-28.7	A	A	I	
30-01	30.4-30.4	A	B	II	
30-02	30.5-30.6	A	A	I	
30-03	30.6-30.7	A	B	II	
30-04	30.7-30.8	A	A	I	
30-05	30.8-31.0	A	B	II	
31-01	31.2-31.4	A	A	I	
31-02	31.4-31.5	A	B	II	
31-03	31.5-31.6	A	B	II	
31-04	31.6-31.7	A	B	II	
31-05	31.7-31.8	A	A	I	
31-06	31.8-31.9	A	A	I	
31-07	31.8-31.8	A	A	I	
31-08	31.9-32.0	A	A	I	
32-01	32.2-32.2	A	B	II	
33-01	33.0-33.0	A	B	II	slope collapse
38-01	38.0-38.1	A	B	II	

Of the high priority landslides, 22 landslides (or slopes) are of rank I (extremely high risk to the road) and 40 are of rank II (high risk to the road). It was determined that a total of 62 landslides (or slopes) should be given high priority for countermeasures. Areas with concentrated high priority landslides are described below.



Figure 4.3.15 shows a distribution chart of the landslides around L/S00 and L/S01 indicating differences in their influences on the road. Figure 4.3.15 (a) shows the hazard rank based on the evaluation score, and (b) shows that for the risk for the road. It can be seen that there are many landslides with a high hazard rank at L/S00. When influence on the road is considered, the risk is high at monitoring sites L/S00-08 and L/S00-09.

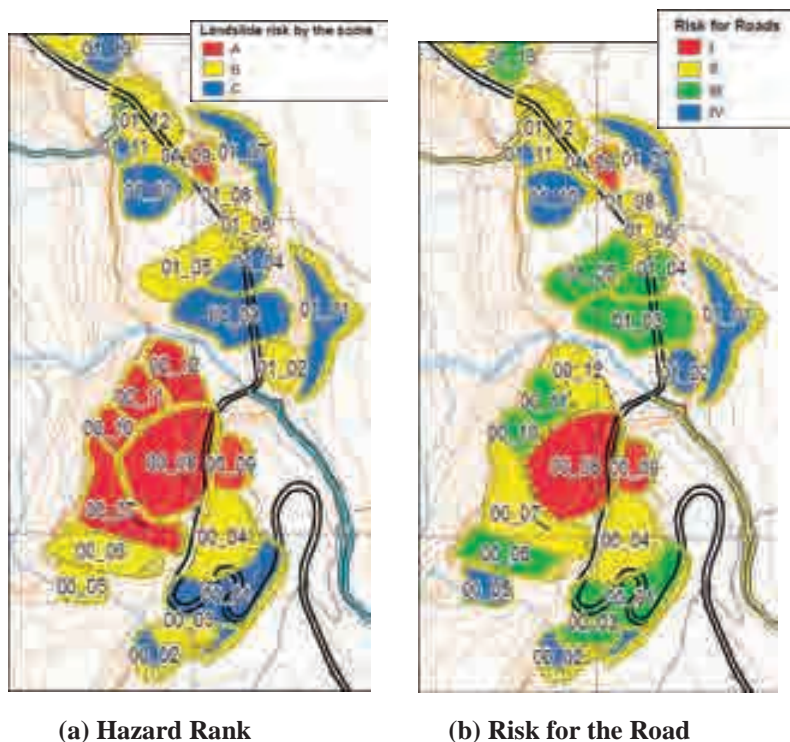


Figure 4.3.15 Area of Particularly High Risk for the Road (L/S00 to L/S01)

Figure 4.3.16 shows the landslide map and photos of L/S00-08. After every rainy season, the depression increases gradually, the gap of the main scarp crossing the road has become larger. As the section of depression of the road corresponds to the L/S00-08 landslide block delineated from photo interpretation and field investigations, this depression is considered to be caused by the landslide movement of L/S00-08. Small scarp of new small landslide appeared at the north side of L/S00-08 head shown in the left photo of Figure 4.3.16.



Figure 4.3.16 Top part of L/S00-08

Figure 4.3.17 shows a distribution chart of landslides around L/S02 to L/S05 indicating differences in their influences on the road. It can be seen that there are many landslides with a high hazard rank around L/S02-06 and L/S05-01. When their influences on the road are considered, there are many (a total of six) high priority landslides such as L/S02-09 and L/S05-01 as showed in Figure 4.3.17 (b).

There are many stepped cracks and currently active landslide blocks (five locations) on the upper portion of the slope at L/S02. Figure 4.3.18 shows a new crack at the head of L/S02-03. There are many new cracks with a maximum step of up to 2m.

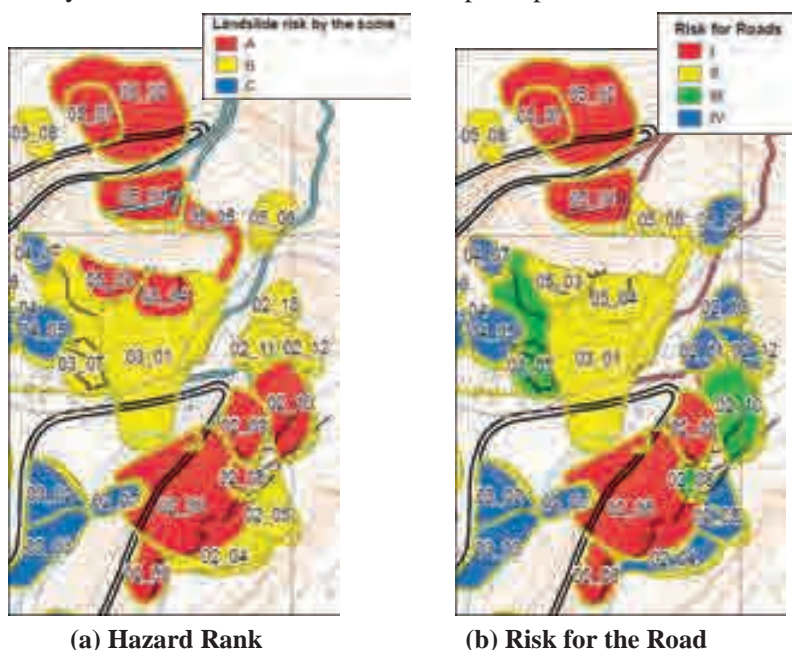


Figure 4.3.17 Area of Particularly High Risk for the Road (L/S02 to L/S05)



Figure 4.3.18 New Cracks at the Head of L/S02-03

Figure 4.3.19 shows new cracks at the head of L/S02-09. These cracks are continuing like a horseshoe-shape, indicating the movement of small blocks in the landslide at L/S02-09. There are other multiple new stepped cracks, so the head of L/S02-09 as a whole may have become unstable.



Figure 4.3.19 New Cracks at the Head of L/S02-09

Figure 4.3.20 shows new cracks at the head of L/S02-10. These cracks are multiple and form small bumps. The multiple steps are small but old landforms, and new cracks exist together. Therefore, this block seems to have activated repeatedly for a considerably long time.

Tremendous damage such as road blockage may occur when many landslide blocks around L/S02 activate on a large scale. Therefore, these blocks have higher priorities among the landslide blocks ranked A in terms of risk for the road.



Figure 4.3.20 View of the Head of L/S02-10



Around L/S05-01, there are many landslides with higher priorities. Figure 4.3.21 and Figure 4.3.22 show landslide blocks on the crown of L/S05-01. Both landslide blocks have many new continuous cracks (three locations in either case), so these landslides are currently activating. The moving mass has piled up at the head of L/S05-01 and collapsed. This is one of the causes for slope failure of L/S05-01. Therefore, for L/S05-03 and L/S05-04, the influence on the road are evaluated as “B” though they are located a long distance from the road. Suppression of the activities of L/S05-03 and L/S05-04 will be one countermeasure against L/S05-01.

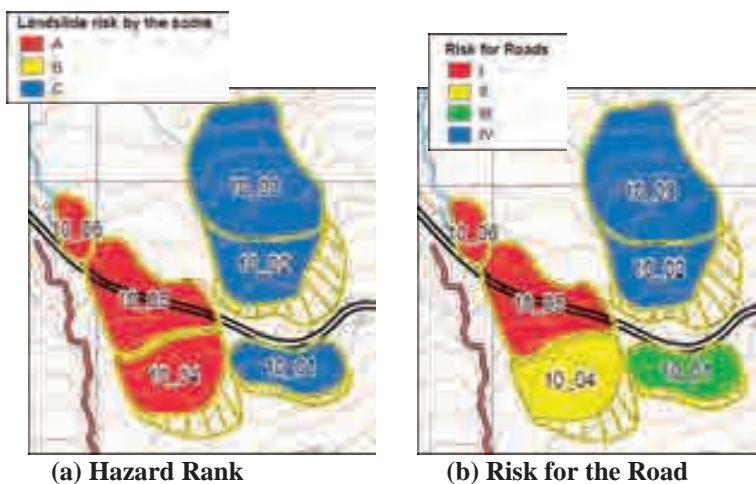


Figure 4.3.21 Landslide Area at L/S05-03



Figure 4.3.22 New Cracks at L/S05-04

Figure 4.3.23 shows a distribution chart of the landslides around L/S10 indicating differences in their influences on the road. The risk is high at L/S10-05, where the deformation of the road is increasing. However, the speed of movement will not change significantly in the future because the slope of the whole area around this landslide is gentle. Therefore, repair of the road once every several years is sufficient.



(a) Hazard Rank

(b) Risk for the Road

Figure 4.3.23 Area of Particularly High Risk for the Road (L/S10)

Figure 4.3.24 shows a distribution chart of L/S10-05 and steps and cracks on the road, and these deformations have become larger year by year. Landslide blocks moving and damaging the road are a little smaller than the landslide blocks interpreted from the satellite images. Considering from the progression of the deformation of the road, the rate of movement of L/S10-05 is approximately 10cm per year.



Figure 4.3.24 Deformation of the road by L/S10-05

Figure 4.3.25 shows a distribution chart of the landslides around L/S26 to L/S28 indicating differences in influences on the road. In this area, there are many small landslide blocks (20 to 30) in a large landslide block. The area has active landslide blocks in multiple layers. Therefore, there are many high priority landslides (11 locations).

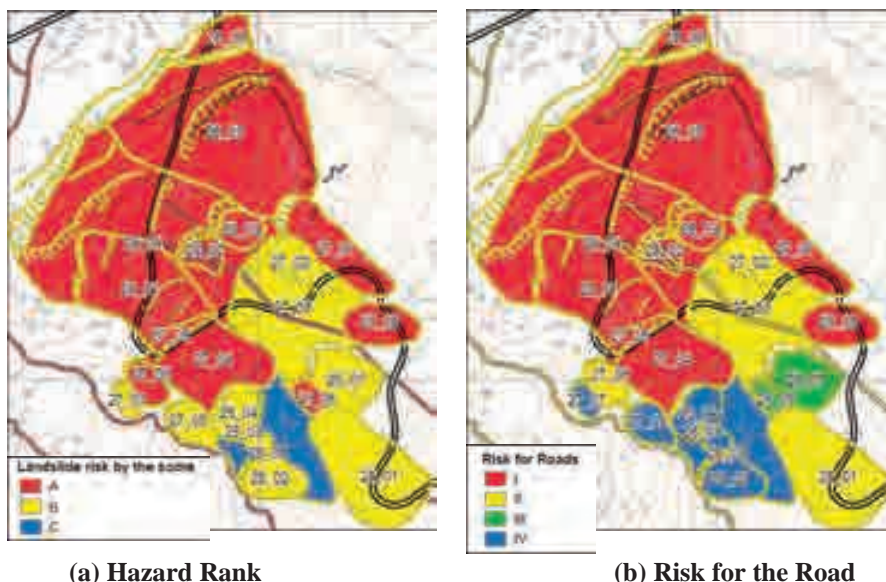


Figure 4.3.25 Area of Particularly High Risk for the Road (L/S26 to L/S28)

Figure 4.3.26 shows the deformation of the side part of L/S26-08. 20 cm steps with left-lateral movement appeared and the deformation is increasing year by year. The ratio of the movement is considered 20 cm or less per year.



Figure 4.3.26 Side crack of L/S26-08

Figure 4.3.27 shows the step on the road by the movement of extending landslide. This step extends to the cracks on cutting slope and under ground of extensometer (EX-5), and the step has become larger year by year.



Figure 4.3.27 Deformation by the extension of L/S27-04

The road near the main scarp at L/S28-05 is deforming continuously. This indicates that L/S28-05 is moving actively. At L/S28-05, the main scarp for the whole block is clear, but the positions of the flanks are not clear. The new stepped cracks on the left flank are shown in Figure 4.3.28. Figure 4.3.28 shows the confluence the left flank and the crack of the subsidence. Figure 4.3.28 shows the uplift on the left flank of L/S28-05. The step on the left flank that continues from the main scarp, which is seen on the left of the figure, clearly reverses in the middle, so the landslide body has been uplifted.



There are signs indicating that these cracks on the flank also expanded recently. Therefore, the whole L/S28-05 block appears to be moving actively. There are multiple continuous stepped cracks in the landslide body of L/S28-05, so there is a trend of dividing into smaller blocks.



Figure 4.3.28 L/S28-05 Left Flank Where Landslide is Clearly Shown at L/S28-05

Figure 4.3.29 shows a distribution chart of the landslides around L/S30 to L/S31 to indicate differences in their influences on the road. The risk is high at locations where the deformation of the road is increasing. However, the displacement rate is small, and the current slow movement will continue. Therefore, repair of the road once every several years is sufficient.

Near L/S31-06, the road deforms on the boundary between the embankment and the slope. A shortage of the strength of embankment may have caused the deformation. The lower portion of the slope may become unstable due to the weakened embankment, inducing a new landslide.

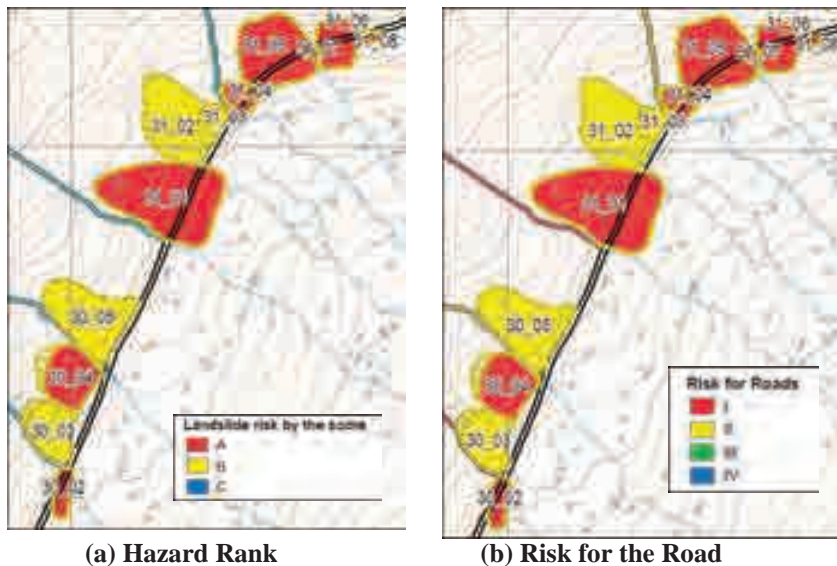


Figure 4.3.29 Area of Particularly High Risk for the Road (L/S30 to L/S31)

Hereinafter, the locations with concentrated high priority landslides will be described. At all monitored sites, the hazard was ranked A. The risk for the road was ranked A or B.

Figure 4.3.30 shows the steps of L/S30-02. Although the step has become larger year by year, only vertical movement and no horizontal movement was observed. Mountain-facing steps can be observed, but valley-facing steps in pairs were not observed. The culvert crosses under the road diagonally, and road bank materials may be discharged/ eroded with leaking water during the rainy season.



Figure 4.3.30 Step of L/S30-02

Figure 4.3.31 shows the deformation of L/S31-04. Steps and lateral slips appeared on the road surface, and a huge basalt boulder pushed out and crashed into the road side ditch. The steps have become larger year by year. Two valley-facing steps, which are 10m apart, can be observed, but no other steps in pairs can be observed on the other side. Similar to L/S30-02, a culvert crosses under the road diagonally, and road bank materials may be discharged/ eroded by leaking water during the rainy season.



Figure 4.3.31 Deformation of the road at L/S31-04

Figure 4.3.32 shows the deformation of L/S31-07. Steps and lateral slips appeared on the road surface, and side ditch is also deformed. The steps have become larger year by year. The valley-facing steps can be observed in the down slope from the road, but no other mountain-facing steps in pair can be observed on the other side. Culvert crosses under the road, road bank materials may be discharged/ eroded by leaking water in the rainy season.

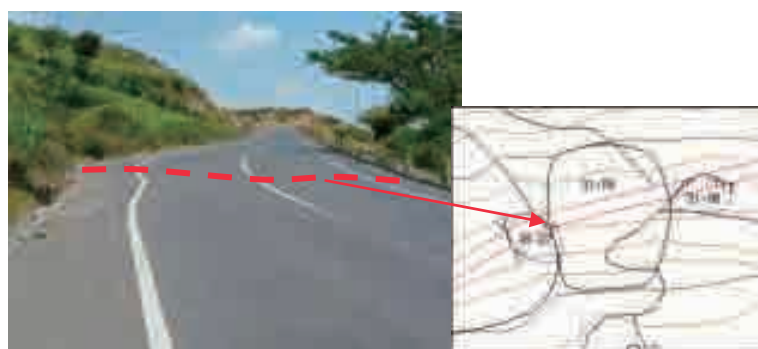


Figure 4.3.32 Deformation of the road at L/S31-07



Figure 4.3.33 shows the deformation of L/S31-08. Steps and lateral slips appeared on the road surface, and side ditch is also deformed. The steps have become larger year by year. The valley-facing steps can be observed in the slope below the road. Deformation of the side ditch can be observed on the mountain side, and a major step ends in the center of the road. The road of the section is built by rock fill, and slight swelling can be observed on the filled road slope. The swelling seems to be caused by weakness of the road fill material and buried landform, such as shallow valley with saturated groundwater. So, the swelling may be a precursor of road slope collapse.



Figure 4.3.33 Deformation of the road at L/S31-08

Figure 4.3.34 shows the deformation of L/S38-01, close to Dejen Town. As steps in pairs can be observed, this section is considered to be a small landslide. Four small deformations and pot holes appeared. The symbol of < shows culvert in the Figure 4.3.34, and most of the deformations appear above the culvert. Some destruction can be observed in the holes of the culverts, discharging water may leak at the points of destruction. According to the phenomena, road bank materials may be discharged/ eroded by leaking water in the rainy season.

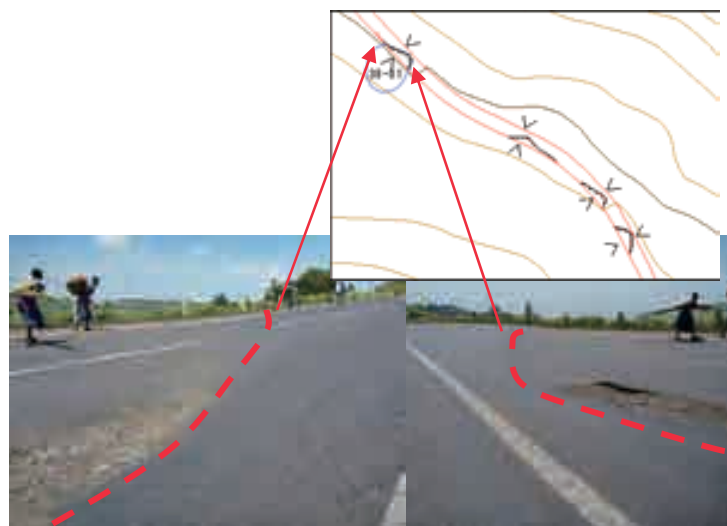


Figure 4.3.34 Deformation of the road at L/S38-01

## 4.4 Landslide Block Interpretation

### 4.4.1 Geological character of landslides by block

In this section, the geology of each landslide block is summarized by the results of geological reconnaissance, the core observation on the drilling operation. The results were summarized as drilling logs and drilling core photos.

#### a. Geology of the landslide in L/S00 (ST.0+200 to 1+100)

The area is located in basalts and pyroclastic rocks representing the Ashangi Formation. The main road was constructed on the bedrocks, and the embankment runs through the boundary of the cliff and the flat plane. Schematic geological column of this area is shown in Figure 4.4.1.








Column	Geology	Remarks	Borehole
	Basalt (1)	Flat plane of Goha Tsiyon village.	BH00-11
	Pyroclastic rock (1)	Sandy tuff to tuffaceous coarse sand. 2-5 m thickness. Flat plane on top of the basalt (2).	BH00-11
	Basalt (2)	Massive with pillow lava. Cliffs on road side.	BH00-11
	Pyroclastic rock (2)	Fine tuff to lapili tuff with mudstone-like tuff. Widely exposed at the road side.	BH00-11
	Basalt (3)	Highly weathered porous basalt. Very soft and brittle.	BH00-12, BH00-21
	Pyroclastic rock (3)	Fine tuff to lapili tuff. As deeper, Fresh rod-like mudstone.	BH00-12, BH00-13, BH00-21
	Basalt (4)	Escarments over 100 m thick below the area. Developed columnar joints	

Figure 4.4.1 Schematic geological column in the landslide in L/S00

#### a.1 Artificial embankment

Artificial backfill embankment is composed of basalt cobbles/boulders (5-60 cm), gravel, sand, mud and clay. The matrix except basalt boulders in the core samples of the drilling operation had been washed away. The thickness of the layer is up to 22 m in this area. Water permeability of the layer is considered to be very high.

#### a.2 Colluvial deposit

Colluvial deposit is mainly composed of basalt cobbles/boulders (5-600 cm), gravel, sand, mud and clay including black and organic soil as “black cotton soil”, which have come from the mountainous side cliff. The deposit overlies on the surface with 0-5 m thickness, and partly intercalated with around 20 m thickness under the artificial embankment. Water permeability of the deposit is considered to be very high.

#### a.3 Basalt (1)

Basaltic lava which is distributed on the uppermost layer of the area is purported as “basalt (1)” in this report. The basalt is widely exposed over 40 m thick. The unit is mainly black to dark grey and has clearly developed vertical columnar joints (20-50 cm) (Photo 4.4.1). Small holes (3-10 mm) by foaming are scattered in the rock. Water permeability of the layer is

controlled by the columnar joints and it is high.

The top surface of the unit forms the flat plane of Goha Tsiyon Village (Photo 4.4.2), and it also shows steep escarpments at the beginning of the Abay Gorge.



Photo 4.4.1 Clearly developed vertical columnar joints in the Basalt (1)



Photo 4.4.2 Flat plane of Goha Tsiyon village

#### a.4 Pyroclastic rock (1)

Pyroclastic rock (1) is intercalated between the upper basalt (1) and after-mentioned basalt (2). The unit is sandy tuff to tuffaceous coarse sand (Photo 4.4.3) with lenticular clayey mud layers. It is very soft and brittle, and is susceptible to weathering and erosion, resulting in a flat plane on top of the basalt (2) (Photo 4.4.4). The color is mainly white to grey which is relatively fresh area and grey to black brown which is highly weathered.

The layer is partly exposed at the area and at 4.5-6.6 m depth of BH00-11. The thickness is around 2-5 m. The strike of the bedding is EW with 10-60 north dipping. Water permeability of the layer is moderate, and the groundwater from the columnar joints of the upper basalt flows out from top of this tuff layer.

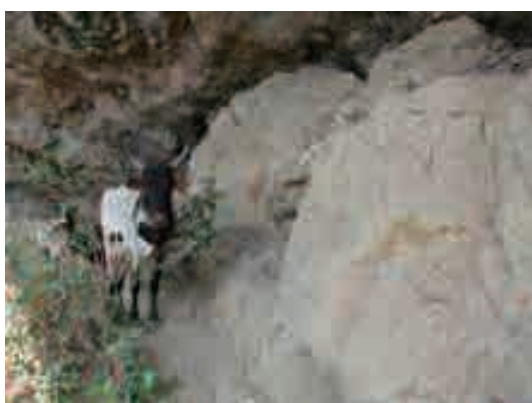


Photo 4.4.3 Sandy tuff to tuffaceous coarse sand with lenticular clayey mud layers



Photo 4.4.4 Flat plane on top of the Basalt (2)

#### a.5 Basalt (2)

This layer is basalt lava. The structure is “massive” which means that columnar joint is little or nothing, and relatively fresh. Spherical structure like pillow lava is observed at top of the

unit (Photo 4.4.5). The fresh part of the unit is bluish grey, whilst the weathered area is grey brown with red brown cracks. Small holes (1-4 mm) by foaming are sparsely scattered at the upper part in the rock. Water permeability of the layer is controlled by the joints and it is high.

Basalt (2) is exposed on the mountainous side and at 6.9-31.8 m depth of BH00-11, and forms cliffs on the main road side. The boundary of the overlying pyroclastic rock (1) is unclear. The thickness is around 5-30 m.



Photo 4.4.5 Spherical structure like pillow lava is observed in the Basalt (2)



Photo 4.4.6 Fine tuff to lapili tuff with partly sandy tuff in the Pyroclastic rock (2)

#### a.6 Pyroclastic rocks (2)

Pyroclastic rock (2) is intercalated between the upper basalt (2) and after-mentioned basalt (3). The unit is fine tuff to lapili tuff with partly sandy tuff (Photo 4.4.6). Mudstone-like tuff with dark grey in color is partly observed as outcrops (Photo 4.4.7) and the core samples. It is susceptible to weathering and erosion, resulting in overhung landform under the basalt (2) (Photo 4.4.8). The top of the unit which is boundary to the basalt (2) is especially soft and brittle because of the contact of basalt lava, which results in rockfall and slope failure. The color is bluish green to black grey which is relatively fresh area and brownish grey to red brown which is highly weathered.



Photo 4.4.7 Mudstone-like tuff with dark grey in color in the Pyroclastic rock (2)



Photo 4.4.8 Overhung landform, which is resulted in by erosion, under the basalt (2)



The layer is widely exposed at the road side and below 31.8 m depth of BH00-11. The thickness is estimated around 30-40 m and becomes thick toward the end point. The bedding plan is unclear in this area. Water permeability of the layer is moderate, and the groundwater from the upper basalt flows out from top of this layer.

#### **a.7 Basalt (3)**

Basalt (3) is obtained under the embankment as core samples of BH00-12 and BH00-21. The layer is considered to be distributed as almost horizontal sheet, which is 2-11 m thick.

The core samples are highly weathered porous basalt with cracks which are red-brown or black in color by weathering. Fractured and weathered parts are mainly composed of clay, sand and gravel. Calcite veins are sparsely found in the core. It is very soft and brittle by weathering. Water permeability of the layer is controlled by the joints and the cracks and it is considered to be high.

#### **a.8 Pyroclastic rocks (3)**

Pyroclastic rock (3) is observed as core samples of BH00-12, BH00-13 and BH00-21. The unit is fine tuff to lapili tuff. The mudstone-like tuff with black in color is observed below 33.9 m depth of BH00-13. As deeper, the core sample gradually becomes fresh rod-like mudstone. Weathered parts are clay, sand and gravel with cracks which are red-brown or black in color by weathering. The color is bluish green to grey which is relatively fresh area and brownish grey to brown which is highly weathered.



Photo 4.4.9 Flat plane on top of the basalt (4)

It is soft and brittle, and is susceptible to weathering and erosion, resulting in a flat plane on top of the basalt (4) (Photo 4.4.9).

#### **a.9 Basalt (4)**

The basalt is widely exposed as steep escarpments over 100 m thick below the area (Photo 4.4.10). The unit is mainly black to dark grey and has clearly developed columnar joints which are mainly horizontal direction (around 20-100 cm) (Photo 4.4.11). The top surface of the unit forms flat plane under this area (Photo 4.4.9), and it is exposed on the river surface next to the landslide site. Water permeability of the layer is controlled by the columnar joints and it is considered to be high.



Photo 4.4.10 The Basalt (4) widely exposed as steep escarpments



Photo 4.4.11 Clearly developed columnar joints which are mainly horizontal direction

### b. Geology of the landslide in L/S05 (ST.4+800 to 5+600)

The area is located around the boundary of the basalts in the Ashangi Formation and the limestone in the Antalo Formation. The main road was constructed on the limestone. Copious amount of debris from the basalt cliff, which affects the road in rainy season, is piled up on the mountainous side of the road. Schematic geological column in this area is shown in Figure 4.4.2. The presumed stratigraphic classification is described as follows.

Column	Geology	Remarks	Borehole
	Basalt	Massive. The phenocryst is small, like mudstone.	
	Tuff (highly weathered basalt ?)	Sand or mud of soft particles prone to liquefying. A few m thickness.	
	Upper limestone	Thick limestone beds and minor intercalation. Steep slopes and escarpments. Pale grey in color.	BH05-11, BH05-21, BH05-31
	Lower limestone	Thick limestone beds and tuffaceous beds. Gentle slopes. Grey white to white in color.	BH05-12, BH05-22, BH05-32

Figure 4.4.2 Schematic geological column in the landslide in L/S05

#### b.1 Colluvial deposit

Colluvial deposit is mainly composed of basalt cobbles/boulders (5-500 cm), gravel, sand, mud and clay including black and organic soil as “black cotton soil”, which have come from the mountainous side cliff (Photo 4.4.12). The deposit is considered to overly on the surface with 0-25 m thickness. The deposit is source of the rockfalls and slope failures affecting the main road, especially in the rainy season.

The upper surface of the deposit is a flat plane, which consists of gravels both basalt and limestone. The limestone gravel is considered to have been brought from other areas because the limestone is exposed on lower parts than there. An old drainage ditch having artificial plastic sheets is located on the deposit (Photo 4.4.13).



Photo 4.4.12 Colluvial deposit which have come from the mountainous side cliff



Photo 4.4.13 An old drainage ditch having artificial blue plastic sheets

## b.2 Basalt

Basaltic lava is distributed on the uppermost layer in the area. The structure is “massive,” which means that there are little or no columnar joints. The phenocryst in the rock is relatively small, and it looks like mudstone (Photo 4.4.14). The fresh part of the unit is dark grey, whilst the weathered area is grey brown with red brown cracks. Water permeability of the layer is controlled by the joints and it is high.



Photo 4.4.14 The phenocryst in the Basalt is relatively small, and it looks like mudstone

The cracks which are considered to be formed by stress release lead to rockfall. The basalt cliff is a continuous source of rockfalls to the area, where the debris is thickly piled up under the cliff.

## b.3 Tuff (highly weathered basalt)

Tuff, which might be highly weathered basalt, is intercalated between the basalt and the limestone (Photo 4.4.15). It is sand or mud of soft particles prone to liquefying in the case of containing water. The color is yellowish brown over time due to oxidation. The layer is very soft and erosive, which would trigger slope collapses (Photo 4.4.16). The thickness is not large and is a few meters at a maximum. Water permeability of the layer is relatively high.



Photo 4.4.15 Tuff, which might be highly weathered basalt, under the Basalt



Photo 4.4.16 The layer is very soft and erosive, which trigger slope collapses

#### **b.4 Upper limestone**

The limestone which is fine to medium grained is widely distributed in the area and is more than 25-40 m thick near the road (Photo 4.4.17). The structure is “massive” which means that there are little or no vertical cracks, and it is relatively fresh. The layer is characterized by thick limestone beds and minor intercalation of silt and marl, which are hard and weak alternative layers. The color of the limestone is pale grey and sometime yellowish grey and brownish grey (Photo 4.4.18).

The layer forms steep slopes and escarpments. Overhangs are formed by erosion around the boundary with the upper tuff, where there is water runoff from the boundary. The bedding plane is generally horizontal. Water permeability of the layer is relatively low, so that vegetation grows on the layer boundary.



Photo 4.4.17 Limestone is distributed more than 25-40 m thick near the road



Photo 4.4.18 The color is pale grey, yellowish grey and brownish grey

#### **b.5 Lower limestone**

The limestone which is fine grained is widely distributed under the “upper limestone”. In general, it is horizontally bedded. The structure is “stratification” which means that it is composed dominantly of alternative layers of thick limestone beds and tuffaceous gravel or clay beds (Photo 4.4.19). The color is slightly grey-white to white. Water permeability of the layer is relatively low.



The hardness is relatively soft to moderate, so that it forms gentle slopes (Photo 4.4.20). The boundary of the “upper limestone” and this layer is forming a flat plane where the main road runs.



Photo 4.4.19 Alternative layers of limestone beds and tuffaceous gravel or clay beds



Photo 4.4.20 The lower limestone forms gentle slope

limestone layer in the lower slope section of Filiklik (Photo 4.4.21). The silt and shale layer is susceptible to weathering and erosion. A part of the shale is totally changed to clay by weathering. These silt and shale layers are not exposed due to weathering and erosion, therefore the silt and shale area shows an almost flat plane and/or gentle slope.



Photo 4.4.21 Reddish and greenish silt and shale layer on the lower slope of Filiklik(STA.11+400)

**c. Geology of the landslide in L/S22 (ST.21+600 to 22+300)**

The area is located on the sandstone in the Adigrat Formation. The main road was constructed on the colluvial deposit/embankment on the sandstone. The collapse of the colluvial deposit would be a trigger of a big road failure. Schematic geological column in this area is shown in Figure 4.4.3. The stratigraphic classification is described as follows.

Column	Geology	Remarks	Borehole
	Colluvial deposit/embankment	Tuffaceous gravel, sandy gravel, mud and clay mixed with basalt, tuff and limestone. 15-20 m thickness.	BH22-11
	Sandstone	Highly consolidated sandstone. Horizontal bedding plane.	BH22-11

Figure 4.4.3 Schematic geological column in the landslide in L/S22

### c.1 Colluvial deposit/embankment

Colluvial deposit/embankment is mainly composed of tuffaceous gravel, sandy gravel, mud and clay. The matrix is mixed with basalt, tuff and limestone. Most gravel is 2-6 cm in diameter, and is sub-angular and angular. The deposit is estimated to overly the base sandstone with a thickness of around 15-20 m.

On this upper slope section, greenish shale is overlying the sandstone layer. This shale layer, so called “lower shale”, is susceptible to weathering and erosion, therefore the shale area shows an almost flat plane or gentle slope with overlying thick colluvial deposits. Under part of this layer contain lots of gravel as a basal conglomerate (Photo 4.4.22).



Photo 4.4.22 Greenish shale and its basal conglomerate.

It may also be distributed on the landslide in L/S22 (ST.21+600 to 22+300) initially.

### c.2 Sandstone

The unit is composed of highly consolidated sandstone, which is fine to medium grained. It is intercalated with mudstone, siltstone shale and conglomerate. One layer is thickly bedded (1-3m) and characterized by thick reddish sandstone and its conglomerate (Photo 4.4.23). The sandstone is basically composed of quartz grain, but sometimes contains reddish fragments, including pinkish or slightly reddish color. The bedding plane is generally horizontal. Water permeability of the layer is considered to be relatively low.



Photo 4.4.23 Thick reddish sandstone and its conglomerate

### d. Geology of the landslide in L/S27-28 (ST.27+200 to 28+800)

The area is considered to be located on the siltstone, the shale and the limestone in the Abay Formation. Landslide activities are frequently observed in this area, especially in the rainy season. Hence the boundary of the base rock, which consists of the siltstone, and the sliding soil mass cannot be clearly identified. Schematic geological column in this area is shown in Figure 4.4.4. The presumed stratigraphic classification is described as follows.



Column	Geology	Remarks	Borehole
	Limestone	Thick limestone beds and tuffaceous beds. Steep cliff including overhung. Grey white to white in color.	
	Silt and shale	Siltstone and shale with limestone mixed with sliding soil mass. Gentle slope. Landslide forms.	BH27-11,12,21,22,23, BH28-11,21,31,32,41

Figure 4.4.4 Schematic geological column in the landslide in L/S27-28

### d.1 Colluvial deposit

Colluvial deposit is mainly composed of basaltic gravel, tuffaceous gravel, sandy gravel, mud and clay (Photo 4.4.24). The matrix is mixed with basalt, tuff, silt, shale and limestone. Most gravel is 2-6 cm in diameter, and is sub-angular and angular. The deposit is estimated to overlie the after-mentioned “silt and shale” with a thickness of around 10-20 m on.

There are several “basalt debris layers” in the colluvial deposit, which are mainly composed of basaltic gravel and basaltic tuff breccia in black grey in color (Photo 4.4.25). The layers are mainly observed at around 1 to 15m depth in the drilling core in the L/S27 block and at around 15 to 25m depth in the drilling core in the L/S28 block. The layers might be related with slip surface in the area, and the detail interpretation is described in Chapter 4.4.5.



Photo 4.4.24 Colluvial deposit composed of gravel, sand, mud and clay



Photo 4.4.25 Basalt debris (upper grey-black cores) in the drilling cores



Photo 4.4.26 The colluvial deposit mixed up with sliding soil



Photo 4.4.27 The limestone forms steep cliff including overhung

The colluvial deposit is mixed up with sliding soil mass in the area where landslides frequently happen, especially in the rainy season; therefore it is difficult to clearly classify the colluvial deposit and the sliding soil (Photo 4.4.26)

### d.2 Limestone

The limestone which is fine grained overlies the after-mentioned “silt and shale” area. In general, it is horizontally bedded. The structure is “stratification” which means that it is composed dominantly of alternative layers of thick limestone beds and tuffaceous gravel or clay beds. It forms steep cliffs including overhangs (Photo 4.4.27). The surface of the



outcrops has been highly weathered and become brittle. The color is slightly grey-white to white. Water permeability of the layer is relatively low.

### **d.3 Silt and shale**

The units are mainly composed of siltstone and shale with minor limestone. These are mixed up with sliding soil mass in the area where landslides frequently happens, especially in the rainy season, therefore it is difficult to classify the sliding soil (Photo 4.4.28).

The siltstone unit is composed of silt/clay particles cemented together. It is found intercalated with shale, mudstone and sandstone with calcite and/or gypsum veins in places. The color is white brown to reddish brown which have been weathered and yellowish green to brownish grey which are relatively fresh. The shale unit is argillaceous clastic sedimentary rock which contains a lot of clay minerals. A part of the shale is totally changed to clay by weathering, which is relatively soft and weak due to weathering.

The layers are susceptible to weathering and erosion, therefore the area shows an almost flat plane and/or gentle slope in the village area (Photo 4.4.29). In this area a gentle slope is formed by removed soil and has lots of landslide forms.



Photo 4.4.28 The silt and shale unit mixed up with sliding soil mass



Photo 4.4.29 The silt and shale layers show flat plane and/or gentle slope



#### 4.4.2 Cross sectional interpretation

Representative geological cross sections for each selected site are prepared on the basis of the geological features of each landslide block in the previous description.

When considering making geological cross sections for landslides, it requires exact geological features of each landslide block. However, basically a landslide body has a huge mass and compared with the mass, the result of drilling and exploration results are only point and/or linear data. Therefore, to fill in the gaps between data, it requires experimental estimation method such as type classification of Landslide (Table 4.4.1: for an exact explanation see attached Landslide manual chapter 3.1.1). Groundwater level estimation depends on topographic features and spring water points (see.Ch4.2.2).

Table 4.4.1 Type classification of Landslide

category		Rock slide(Rock glide)	Weathered rock landslide	debris like material landslide	Clayey soil landslide
feature					
Plain figure		horseshoe-type chine type	horseshoe-type chine type	horseshoe-type, chine type, stream type, bottle neck type	stream type bottle neck type
Micro topography		convex ridge	convex table land single-mound depression table land	multi-mound depression table land	depressional gentle slope
Type of slip surface		chair form, ship form	chair form, ship form	step form, stratiform	step form, stratiform
Old classification		young stage	adolescence stage	stage of maturity	old stage
major feature of sliding soil mass	top part	fresh rocks, rarely weathered rocks	weathered rocks with cracks	earth and sand with gravel	boulder or earth and sand with gravel
	toe part	weathered rocks	soil with boulder	earth and soil, partly argillation	clay or clay with gravel
moving velocity		more than 2cm/day	around 1.0 to 2.0cm/day	around 0.5~1.0cm/day	less than 0.5cm/day
continuity of movement		short term accidental movement	certain degree of successive movement (one time per several decad to several century)	successive movement (one time per around 5 to 20 years)	successive movement (one time per around 1 to 5 years)
Slip surface feature		Block slide (chair form)	Translaational slide(Top and toe part indicate partly rotational figure) .	It indicate rotational or translational slide (Toe part are fluidizations) .	Most of Landslide mass indicate translational movement as a thick viscous fluid, but the main scarp is indicate rotational figure.
Blocked state		At first, it indicate single block in usual	It divide to some subdividing small blocks, as secondary landslide, in end part and side part.	It successively divide to small blocks and the landslide mass are almost become earth and soil with gravels.	The landslide mass were totally divided in small block or small part, and move as a thick viscous fluid in mutually related.
Predictability		Almost impossible.It's require detail exploration and close investigation.	It is possible to find on topographical map(1/3,000~1/5,000) and aerial photo.	It is possible to find on topographical map(1/5,000~1/10,000), and the interview from resident people are informative and helpful.	It is easily findout by interview from resident peoples. And it's easily recognize on field.
Common slope figure		It usually had unintelligible platform. Mainly occurred on saddle of mountain ridge which like axes of convex slope.	It clealy had step figure and bond like subduction zone. In exterior view, concave land topography but main part are convex land topography.	It had clear main scarp and under the scarp that had concave land as a pond and swamp, and sometime indicates residual hills. This type of topography mainly made on concave land	On the top of mountaine still remain unintelligible platform. And main part had a equable gentle slope and/or stream like slope.
dominant cause		grand-scale engineering work, clogging action of slope, earthquake, heavy rainfall	heavy rainfall, abnormal snowmelt, streamside washout, earthquake, medium-scale engineering work, other	snowmelt, tropical cyclone, local heavy rainfall, engineering work, other	heavy rainfall, snowmelt, streamside washout, deposited snow, small-scale engineering work
Major geology and structure		It's affected by faults and fracture zone in many cases.	This kind of landslide widely distributed in crystalline schist zone and Tertiary sysytems.It's affected by faults and fracture zone.	This kind of landslide widely distributed in crystalline schist zone and Tertiary sysytems.	This kind of landslide most dominantly in Tertiary systems, and sometime in other fracture zone.

Figure 4.4.5 describes the relation that geological succession and landslide setting on the upper slope of Abay Valley and the geological cross sections are displayed in the following figures

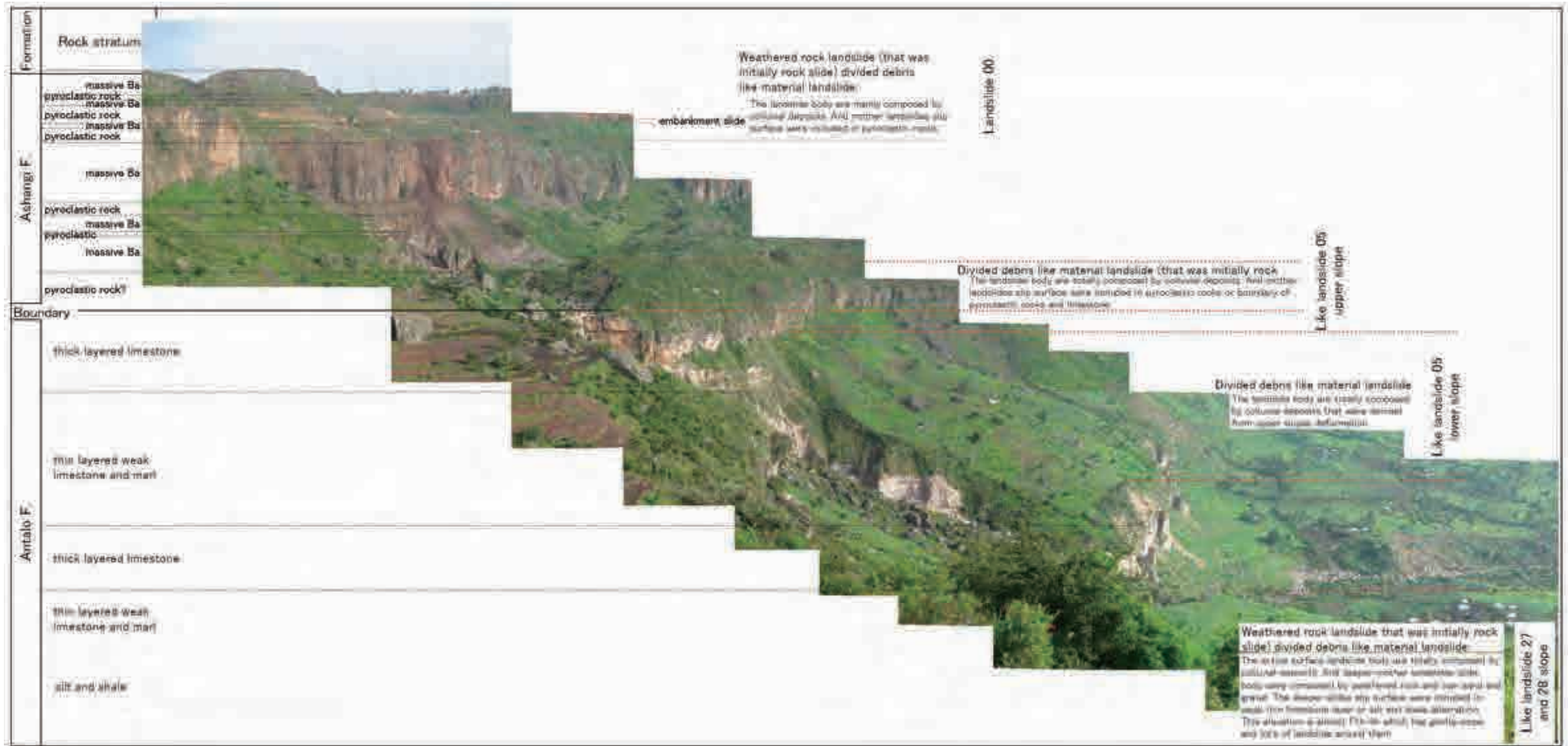


Figure 4.4.5 The relation of geological succession and landslide setting on the upper slope of Abay Gorge.

### a. Geology of the landslide in L/S00 (ST.0+200 to 1+100)

In this area, three kinds of landslide classification were exposed. The biggest one is a weathered rock landslide that was initially a rockslide. This landslide body is mainly composed of colluvial deposits. And its slip surface was within a pyroclastic rock layer. The slip surface was observed as slickenside in pyroclastic mudstone layers core sample for this project. This block's main scarp and topographic features had already almost disappeared so this block was estimated to be in an almost stable condition.

Second landslide was a part of a former landslide. This block is classified as a debris movement of past landslide materials, and is composed of colluvial deposits. These deposits contain sand and soil to huge boulders that are over 5m in diameter. That's why, it is too difficult to find slip surface from the core samples. This block's toe was observed at the 00-07 block's scarp on field observation, and the depth of the slip surface is estimated from the inclinometer monitoring result. The geophysical exploration results and estimation by type classification were used to fill the gap between both of these results.

The most active block was an embankment partial slide. The reasons for the landslide are not only groundwater level difference caused by rain, but also unstable condition of the ground. However, the main trigger is groundwater level rising, so during the dry season road deformation almost stopped. The embankment part is mainly composed of sand and gravel. That is why the water permeability is relatively high and the groundwater level monitoring results show hardly any change.

The location of the geological cross section is shown below.

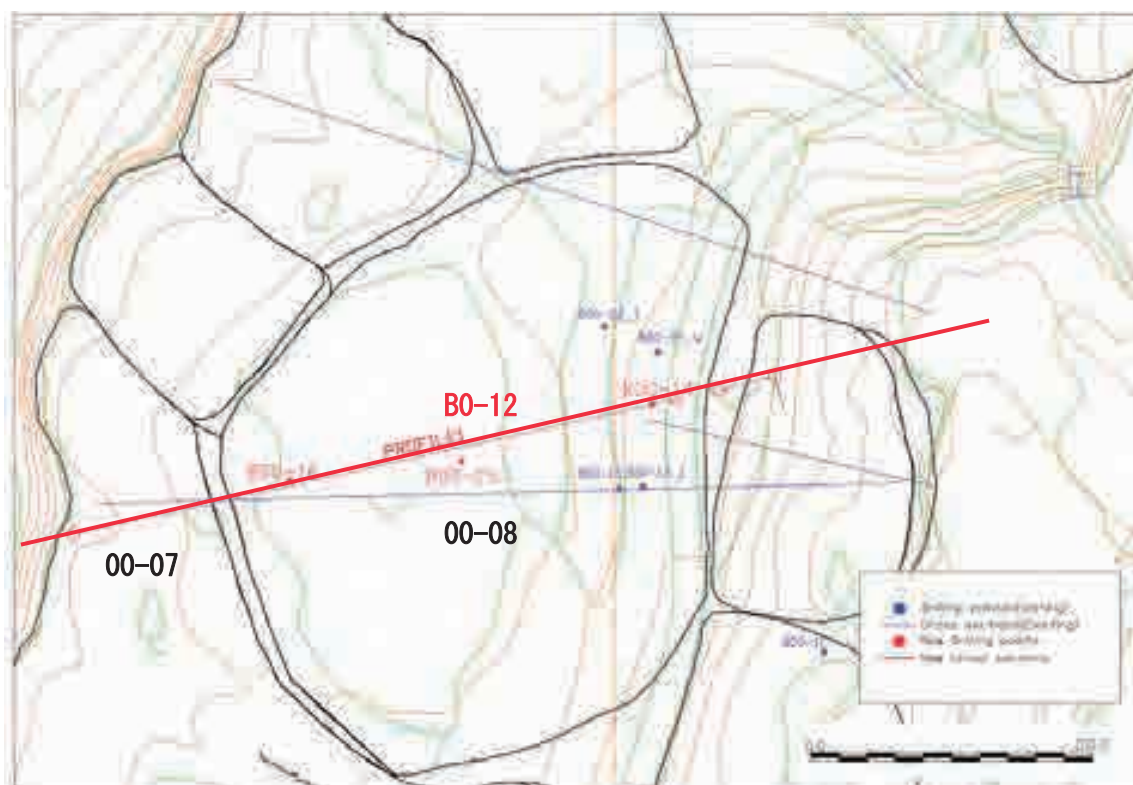


Figure 4.4.6 Survey locations in L/S00



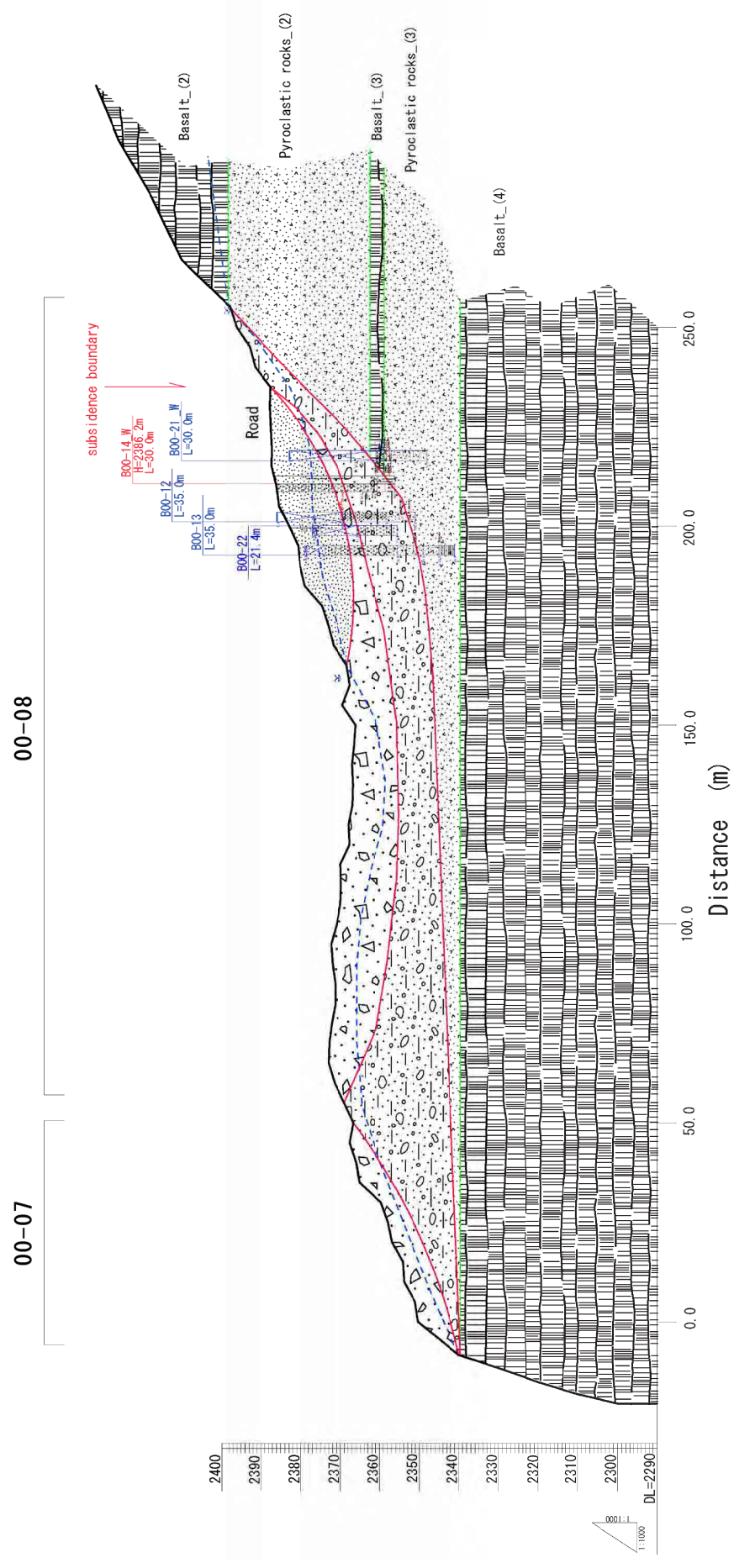


Figure 4.4.7 Geological cross section in L/S00 (B0-12)



## b. Geology of the landslide in L/S05 (ST.4+800 to 5+600)

In this area, two kinds of landslide were identified. Landslide 05-01, located on the upper slope, is classified as a debris movement of past landslide materials. It was initially a rockslide during basaltic material and limestone. And the other (05-02, 05-07) located on the lower slope were classified as debris material landslide derived from upper slopes colluvial deposits.

The landslide 05-01 body is totally composed of colluvial deposits. And the mother landslide's slip surface is within pyroclastic rocks or boundary of pyroclastic rocks and limestone. The area could not be entered by the drilling rig in this study, that's why previous study results of 2007 were used for estimation. This landslide is considered a rockslide initially, so the sliding surface estimated along the boundary of basaltic material and limestone, from the boundary on the road slope and previous drilling results.

The landslide 05-02 and 05-07 are totally composed of colluvial deposits. The landslide 05-07, which is a small block within Landslide 05-02, is the most active part of this lower slope landslide. The landslide shape is estimated by aerial photograph interpretation and reconnaissance. The monitoring results are used for the slip surface estimation. The type classification of these landslides fills a gap between both these results. These landslides are considered to be debris movement of past landslide materials, that's why the slip surface is estimated as an arc like shape.

The location of the geological cross section is as below.

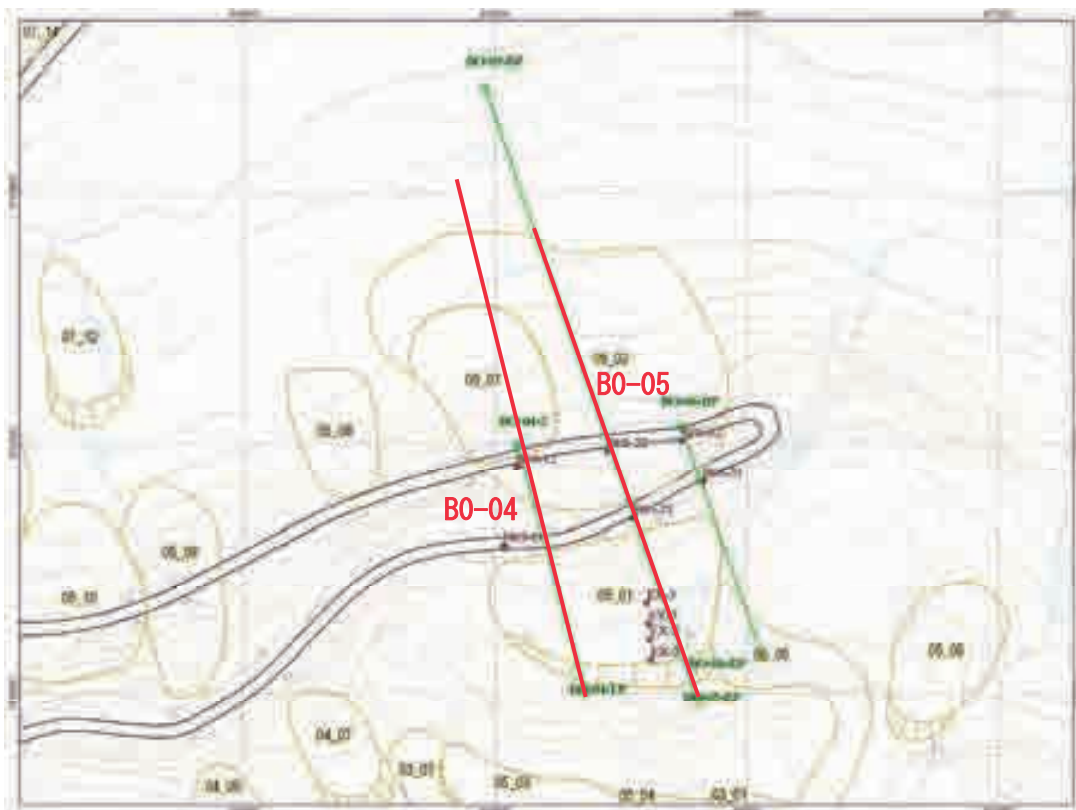


Figure 4.4.8 Survey locations in L/S05

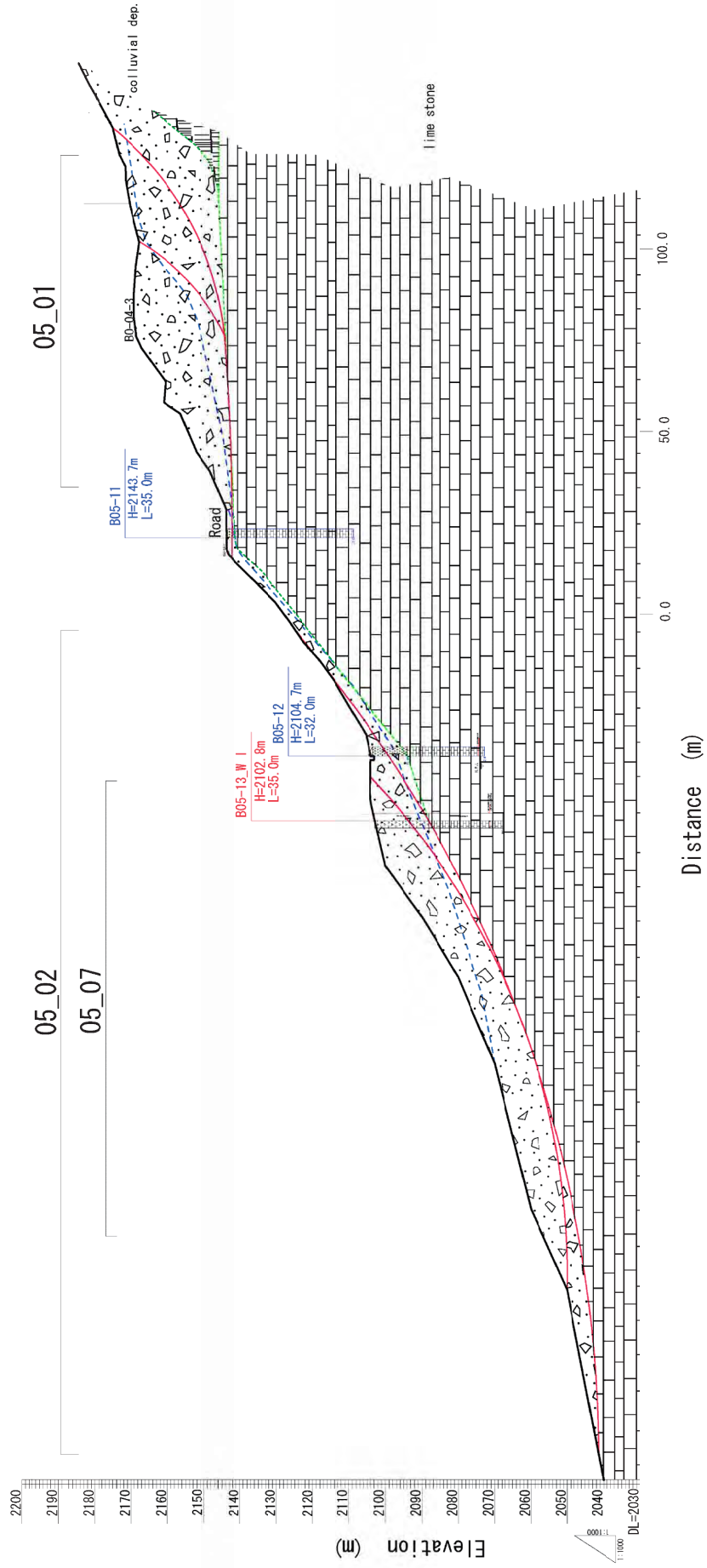


Figure 4.4.9 Geological cross section in L/S05 (B0-04)

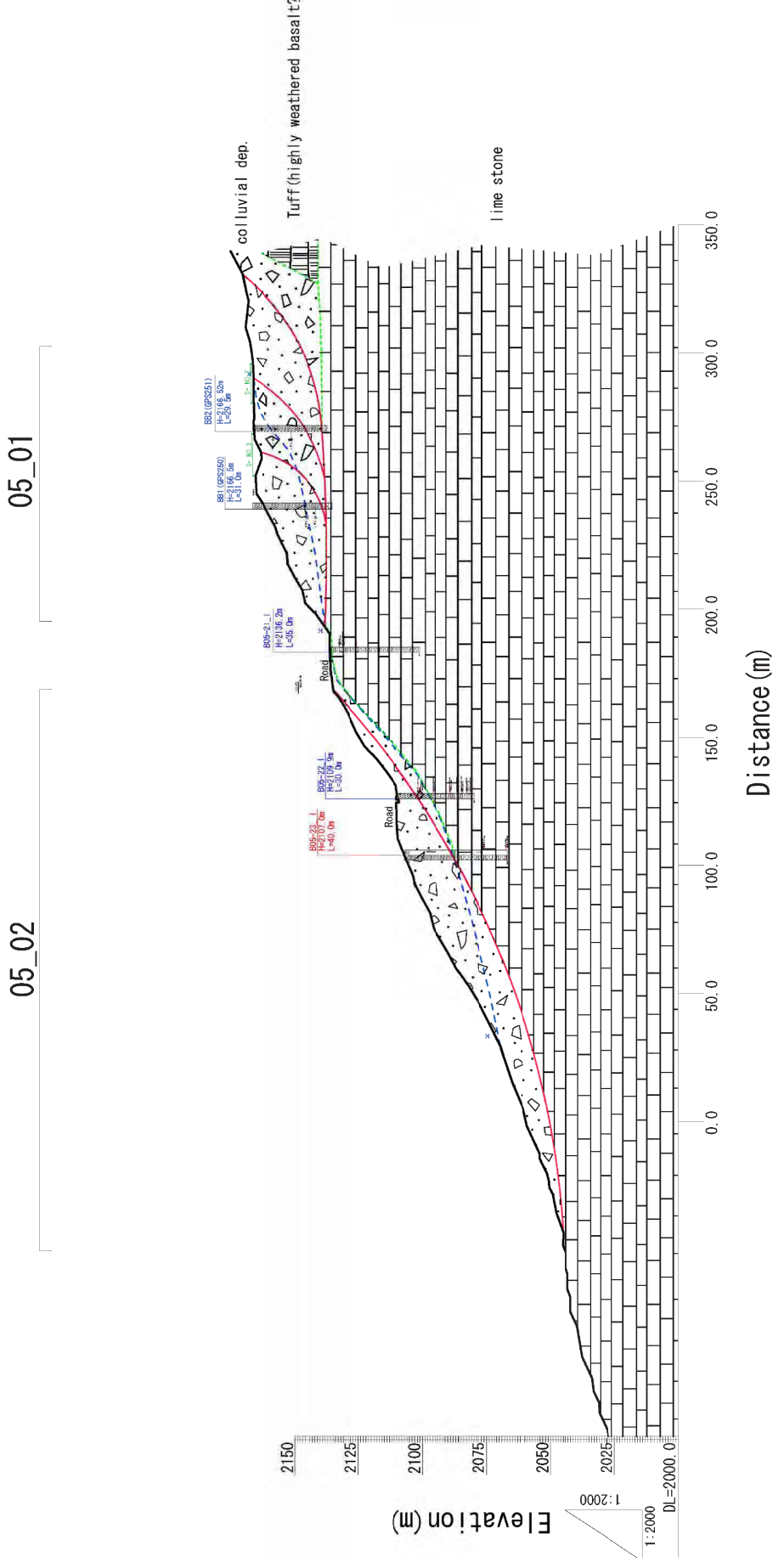


Figure 4.4.10 Geological cross section in L/S05 (B0-05)

### c. Geology of the landslide in L/S27-28 (ST.27+200 to 28+800)

In this area, two kinds of landslide were classified. Initial landslide is classified as weathered rock landslide that is considered as initially rockslide and debris movement which covered the entire landslide area of L/S27-28. In this area, the basement rocks are not exposed due to weathering or erosion, and are covered by colluvial. Therefore the area is mostly flat planes and/or gentle slopes.

The active surface landslide bodies are totally composed of basaltic and/or limy soil and gravel as colluvial deposits. These landslides mainly affected the road. This kind of landslide is too difficult to recognize the slip surface from the core samples, so it requires the monitoring results and geophysical explorations. The aerial photograph interpretation and reconnaissance used to estimate each landslide. The type classification of these landslides fills a gap between both these results.

The deeper mother landslide bodies were composed of soil and gravel derived from “upper limestone” and disturbed silt and shale layer colored greenish grey to reddish brown. The slides slip surface is within a weak thin limestone layer or silt and shale alternation, and non disturbed silt and shale and sandstone were observed under the slip surface. The landslide area was estimated by aerial photograph interpretation.

The location of the geological cross section is shown below.

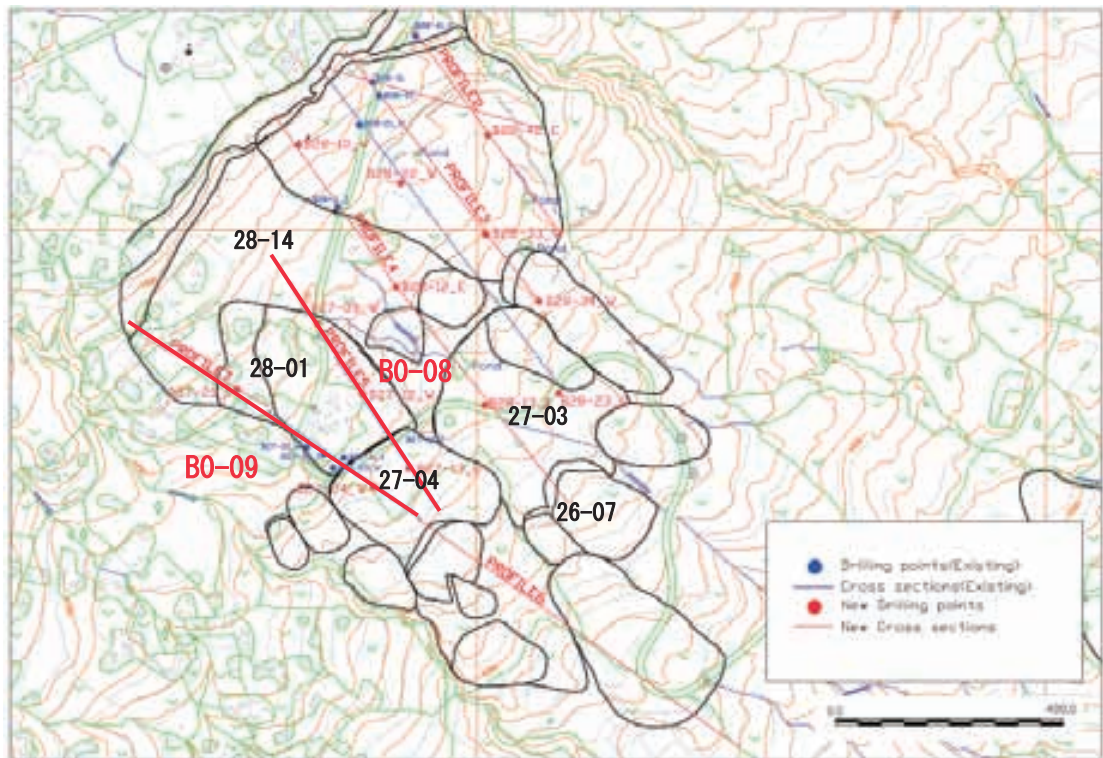


Figure 4.4.11 Survey locations in L/S27



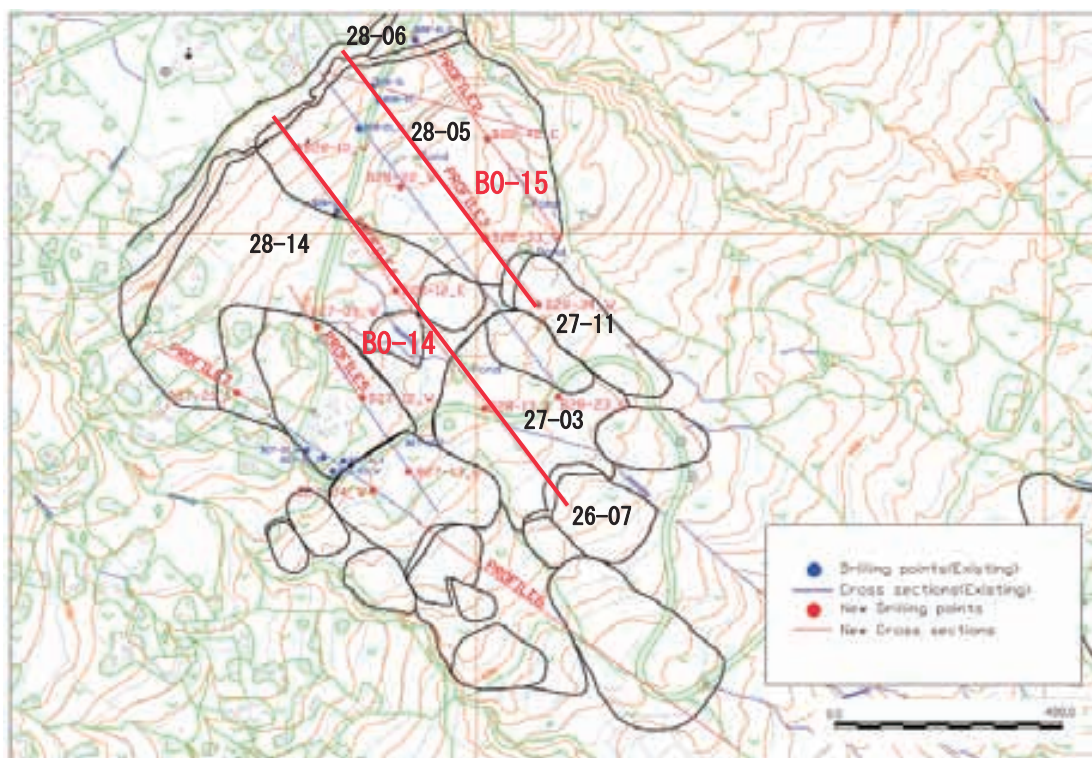


Figure 4.4.12 Survey locations in L/S28

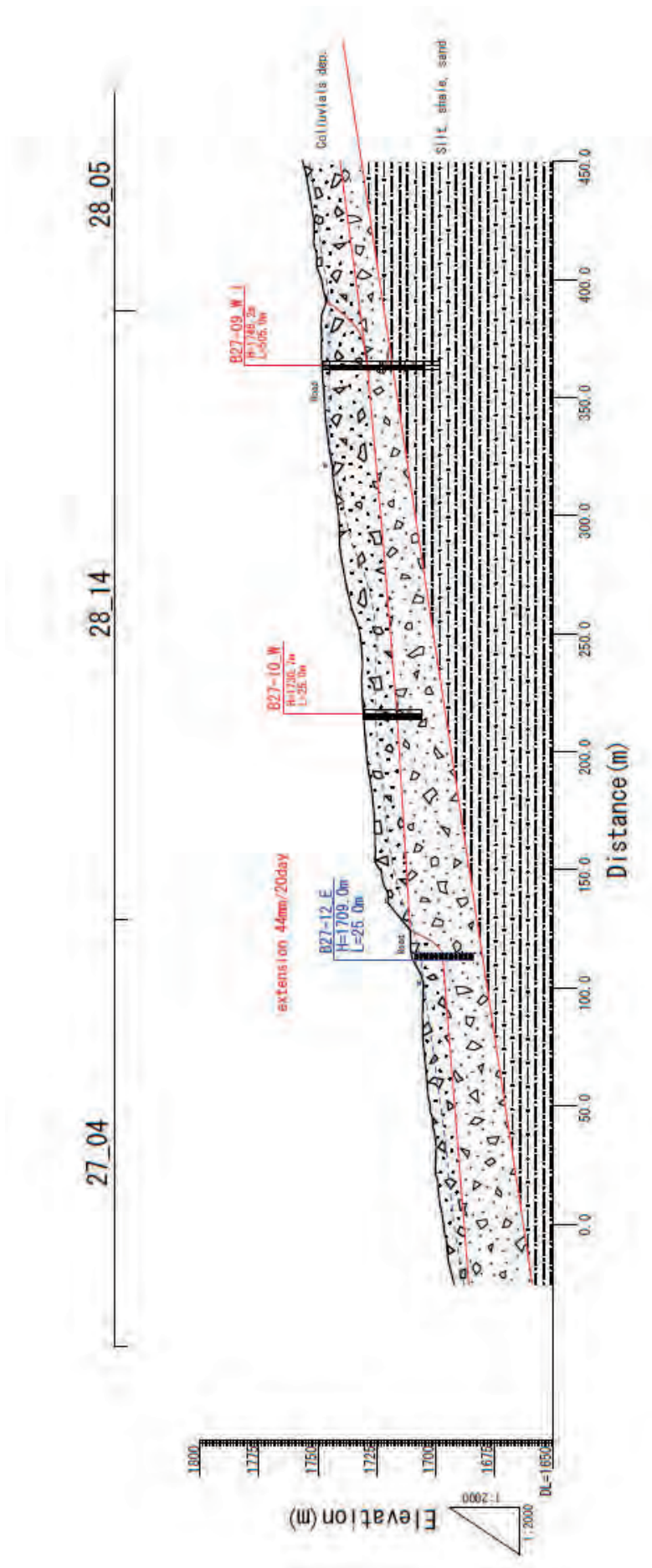


Figure 4.4.13 Geological cross section in L/S27/28 (B0-08)

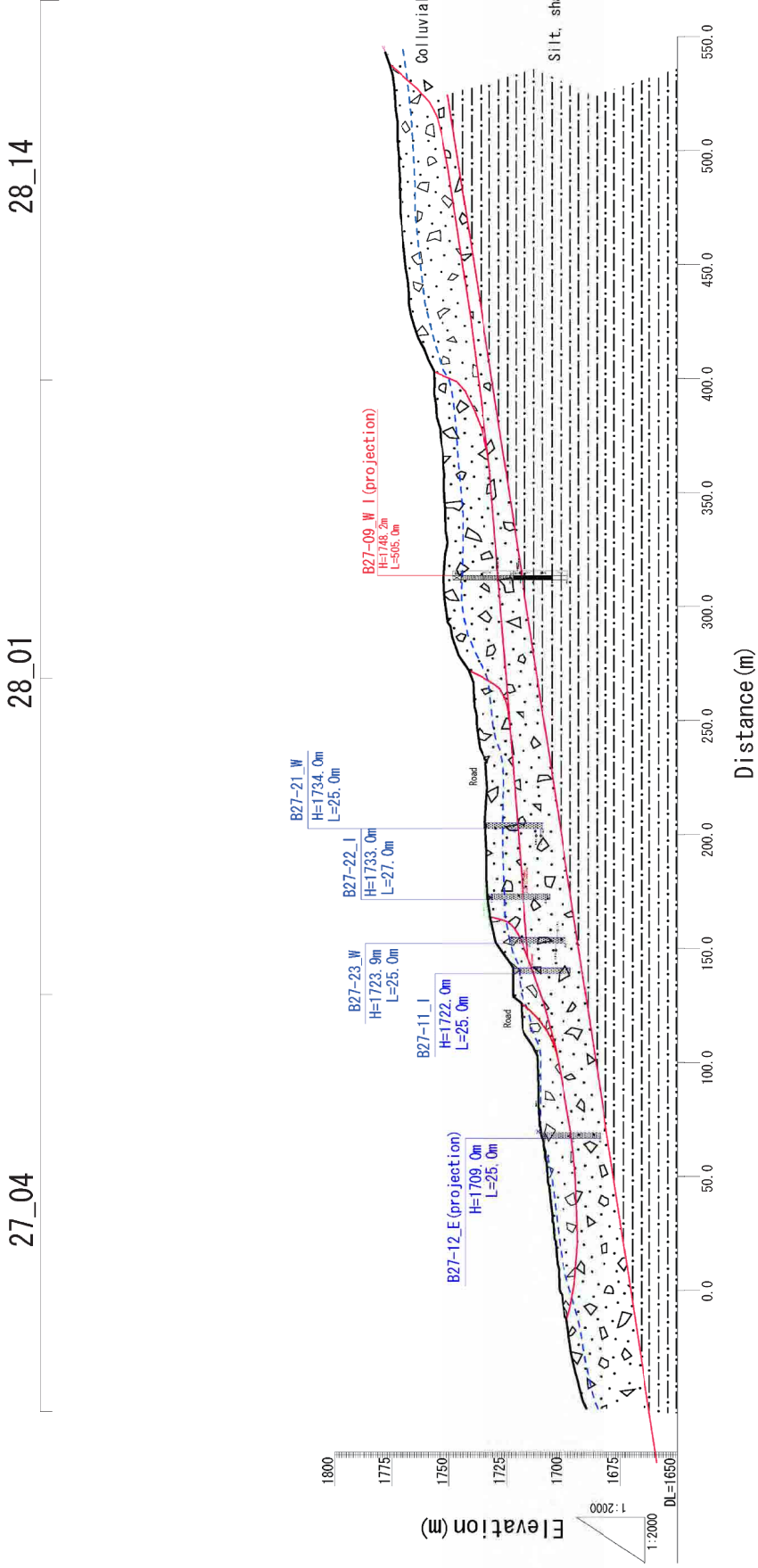


Figure 4.4.14 Geological cross section in L/S27/28 (B0-09)



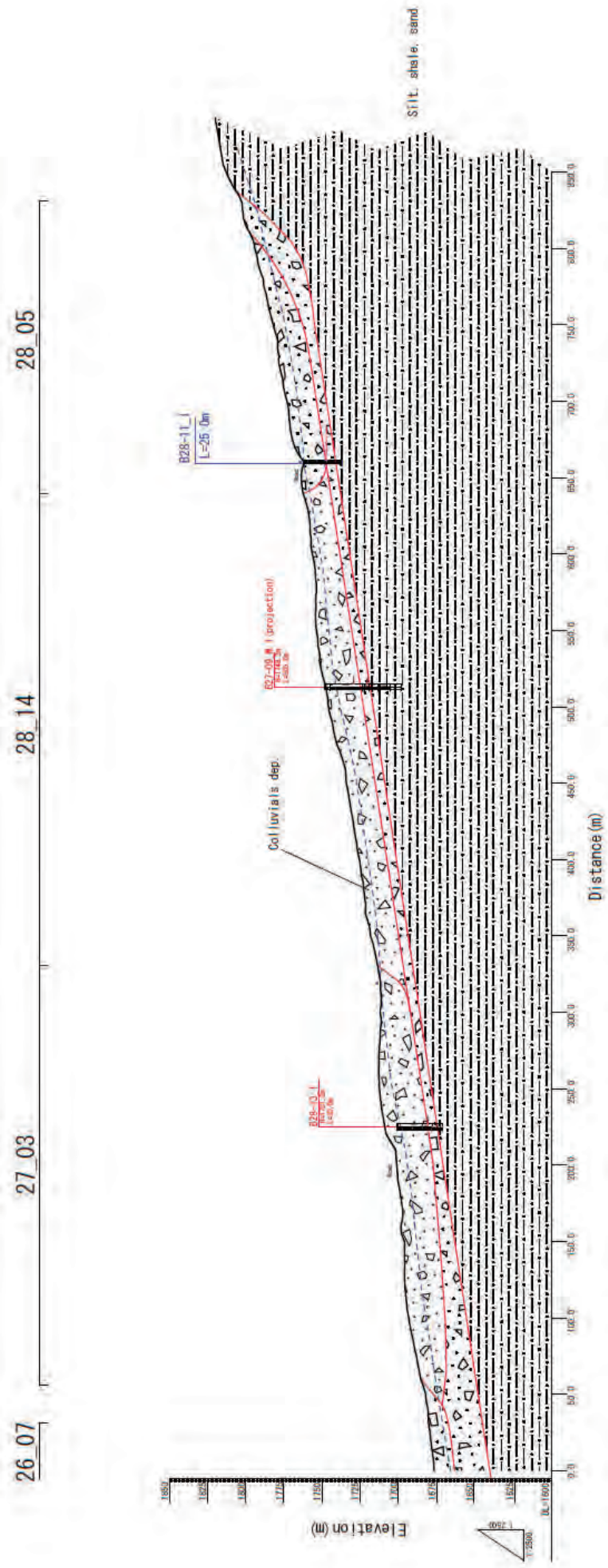


Figure 4.4.15 Geological cross section in L/S27/28 (B0-14)



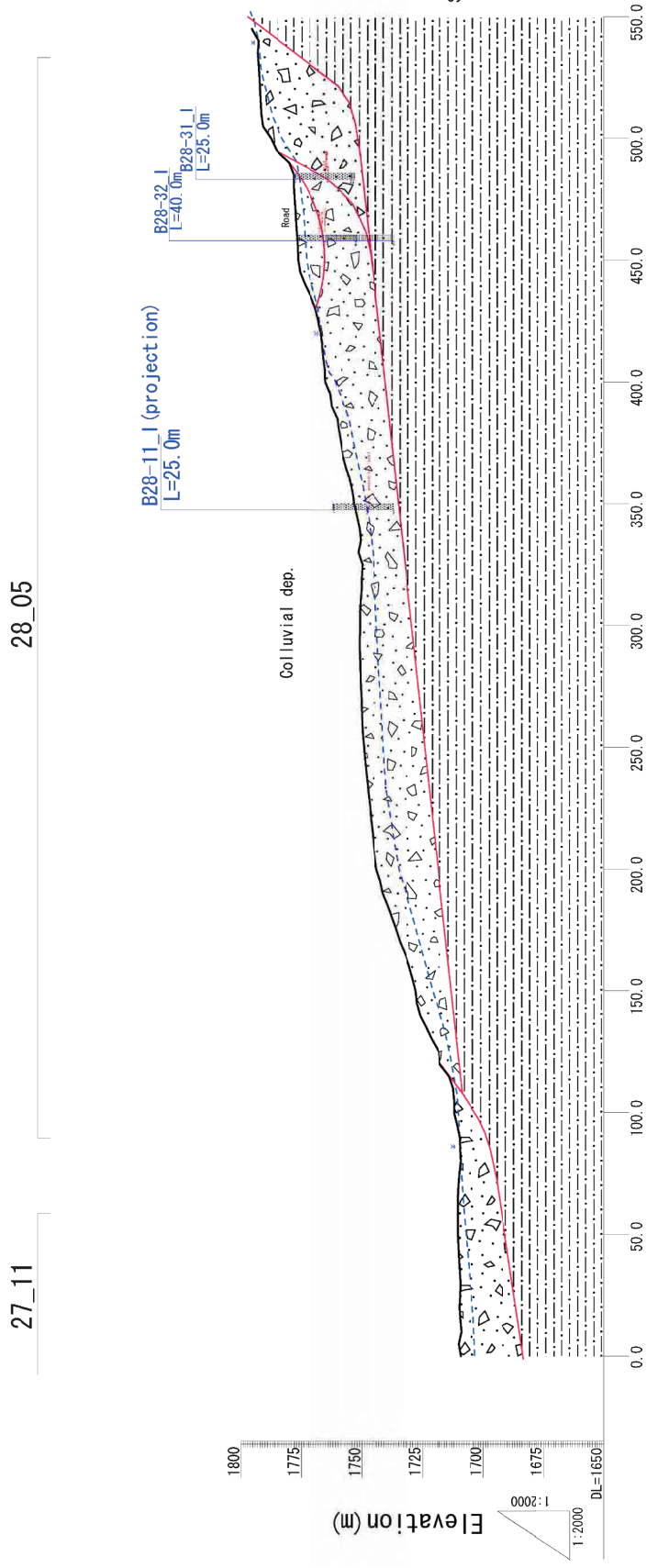


Figure 4.4.16 Geological cross section in L/S27/28 (B0-15)

#### 4.4.3 Monitoring data interpretation

The results of the observation and monitoring with the equipment which was installed in 2010 and 2011 are summarized in this section. The assumed activities of the landslides were examined. It is vital to continue the monitoring to accurately identify the movements of the landslides. The monitoring equipment which was installed is extensometer, borehole extensometer, borehole inclinometer and water level meter. The location maps of the installed equipment are shown in Figure 4.4.17 to 4.4.21.

The outline result of the monitoring with the equipment is shown in the following table, and the detailed results are attached in Appendix. The monitoring data interpretation for each landslide block is described as followed.

Table 4.4.2 Outline of the monitoring results

Location	Extensometer		Borehole extensometer		Borehole inclinometer		Water level meter	
L/S00	EX-1	42.4mm (Compression 26.6mm)	B00-11	0.1mm	B00-12	16.2m	B00-14	-23 to -24m Highest-22.7m
					B00-22	10.5m	B00-21	-20 to -23m Highest-18.1m
L/S05	EX-2	45.5mm (Compression 1.9mm)	B05-11	7.5mm	B05-13	12.5m (minute movement)	B05-12	-31 to -32m Highest-30.9m
					B05-21	7.5m (minute movement)		
	EX-3	57.6mm (Compression 3.8mm)			B05-22	11.0m (minute movement:29.0m)	B05-31	-22 to -23m Highest-21.8m
					B05-23	17.0m (minute movement:30.0m)		
L/S22					B22-11	18.0m (minute movement:5.5m)		
L/S27	EX-4	99.2mm (Compression 0.9mm)	B27-12	48.9mm	B27-09	GL-19.2m measurement impossibility	B27-09	-15 to -16m Highest-15.0m
					B27-11	8.9m		
	EX-5	415.2mm			B27-22	15.4m	B27-21	-22 to -24m Highest-21.9m
L/S28	EX-6	294.9mm (Compression 0.1mm)	B28-41	0.1mm	B28-11	14.7m	B28-21	-20m Highest-20.0m
					B28-13	GL-9.6m measurement impossibility		
					B28-31	14.0m	B28-23	-15 to -17m Highest-14.7m
					B28-32	24.5m		

##### a. Location L/S 00

At extensometer EX-1 installed on gentle slope on the top of the basaltic escarpment, 42.4 mm extension movement on early October 2010 was monitored; however, this value has the possibility by an artificial one or impact. 26.6mm compression movement was observed on

middle March 2011.

The cracks in the area extend in the rainy season and compress in the dry season. The movement (opening and closing) of the cracks in this block, therefore, is considered to be notably related with the precipitation (and/or the temperature). The further discussion about the movement of the cracks on the block will be needed with the continuous monitoring.

At borehole extensometer B00-11 installed on gentle slope on the top of the basaltic escarpment in August 2010, there has been no movement even throughout the rainy season. It is considered, therefore, that there are no landslide activities above 50m depth. Continued monitoring is required for confirmation.

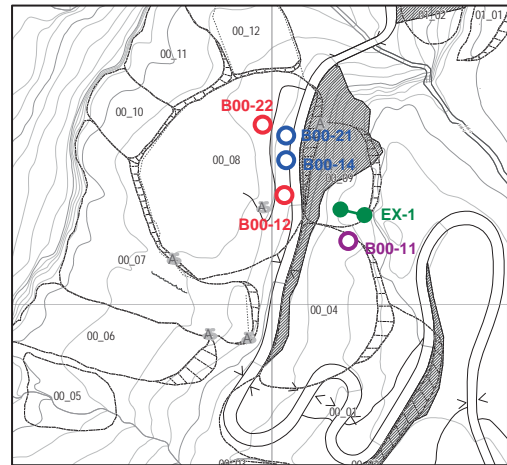


Figure 4.4.17 Location map of monitoring devices in L/S00

At borehole inclinometer B00-12 installed on the roadside on July 2010, the casing pipe was broken by the movement of the landslide at 16.2m depth in August 2010. The measurement has not been implemented since October 2010 because of the breaking of the pipe. At borehole inclinometer B00-22 installed on downside of the road, the measurement has not been able to be implemented since the collapse of the borehole at 10.5m depth when the casing pipe was installed in the middle of October 2010. Not only the broken pipe but the collapsed borehole is attributed to landslide movement, so that it is considered that there are slip surfaces around these depths accompanying active landslide movement.

At water level meter B00-14 (30m depth) installed on the roadside in 2011, the steady water level keeps about -23 to -24m after July 2011. At water level meter B00-21 (30m depth) installed on the roadside, the steady water level of -20 to -23m and the high water level of -18.1m from August 2010 to September 2010 were recorded. The steady water level keeps about -20m after October 2010. Continued monitoring is required for confirmation.

#### b. Location L/S 05

At extensometer EX-2 installed the upper part on the gentle slope, 45.5 mm extension movement during middle August to end of September 2010 was monitored, in contrast to little movement in the dry season. At extensometer EX-3 installed around the channel of the lower part on the gentle slope, extension movement started in middle August and is occurring not only in the rainy season but in the dry season as well, and the extension movement has become 57.6mm. It is considered, therefore, that the landslide activates in the rainy season and is continuously moving even in the dry season in the lower part near the road.

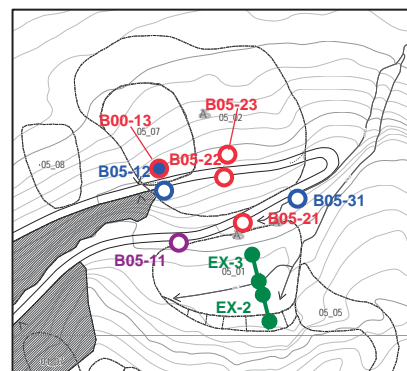


Figure 4.4.18 Location map of monitoring devices in L/S05

At borehole extensometer B05-11 installed on the roadside, 7.1mm extension movement during early September to late November 2010 was monitored. It reached 7.5mm on November 2010. However, movement hardly appears after that.

At borehole inclinometer B05-13 installed on the downward roadside on July 2011, minute movement at around 12.5m depth are observed. Continued monitoring will make clear slip surface in the area. At borehole inclinometer B05-21 installed on the upward roadside, small movement at around 7.5m depth and minute movement at around 29.8m depth are observed. The measurement has not been implemented since November 2010 because of the breaking of the pipe. Similarly, at borehole inclinometer B05-22 installed on the downward roadside, small movement at around 11.0m depth and minute movement at around 29.0m depth are observed. At borehole inclinometer B05-23 installed on the downward roadside on July 2011, landslide movement at 17.0m depth and minute movement at around 29.0m depth are observed. Continued monitoring will make clear slip surface in the area. It is considered, therefore, that active landslides are around both the upward road and the downward road.

At water level meter B05-13 (35m depth) installed on the downward roadside in July 2011, the data has not been recorded since the installation because there has been no water in the hole. At water level meter B05-12 (32m depth) installed on the downward roadside in September 2010, the steady water level -31 to -32m and the high water level -31.0m at August 15 was recorded. However, the data has not been recorded since October 9 because there has been no water in the hole. At water level meter B05-31 (35m depth) installed on the upward roadside in September 2010, the steady water level of -22 to -23m and the high water level of -21.8m on September 2011 were recorded.

### c. Location L/S 22

At borehole inclinometer B22-11 installed on September 2010, minute movement at around 5.5m depth is observed, and the bending of pipe occurred around 18m depth in February 2011. It is considered, therefore, that landslide is confirmed around this area. Continued monitoring is required for confirmation.

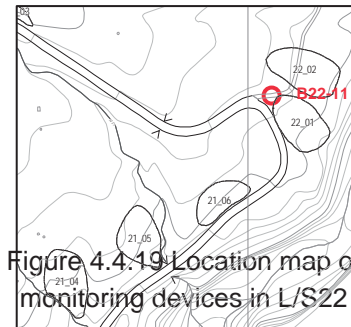


Figure 4.4-19 Location map of monitoring devices in L/S22

### d. Location L/S 27

At extensometer EX-4 installed the upper slope of the road, 50mm extension movement during the middle of August to early October 2010 was monitored, and the movement reached 99.2mm in beginning of October 2011. At extensometer EX-5 installed next to a church, extension movement started in early July and was continuously occurring until late November 2010, and the extension movement reached around 150mm on November 2010. The movement continuously extends even in the dry season and re-activated on August 2011, and it reached 415.2mm in the beginning of October. It is considered, therefore, that the landslide intensively activates in the rainy season and is continuously moving even in the dry season.

At borehole extensometer B27-12 installed on the roadside at the end of September 2010, there had been no movement until on middle August 2011. However, it extended to 48.4mm since August 16 after the heavy rain recorded 244.5mm/day on previous day. The movement hardly appears after that. It is considered, therefore, that the landslide activates with



concentrated heavy rain and is continuously moving even in the dry season. Continued monitoring is required for confirmation.

At borehole inclinometer B27-09 installed on the roadside in July 2011, the measurement has not been able to be implemented since the first measurement because the bending of pipe occurred at around 19.2m depth. At borehole inclinometer B27-11 installed on the roadside in October 2010, the measurement has not been able to be implemented since November 2010 because the bending of pipe occurred at around 8.3m depth.

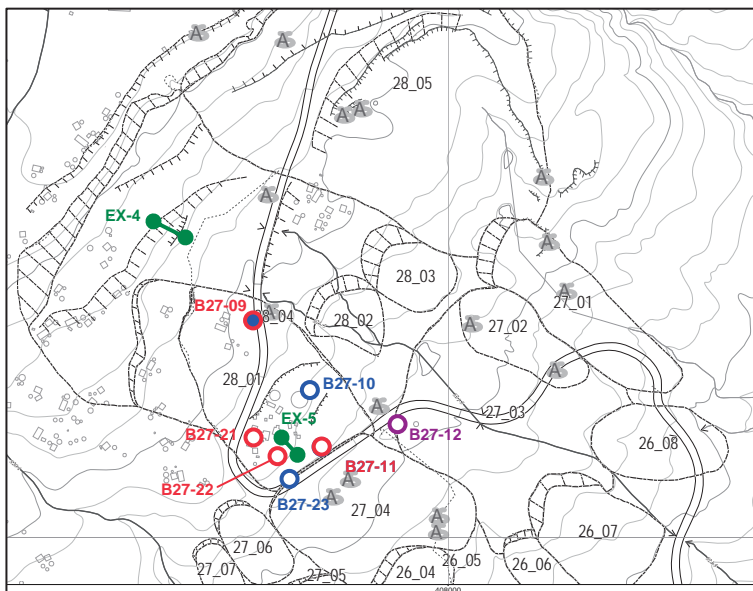


Figure 4.4.20 Location map of monitoring devices in L/S27

At borehole inclinometer B27-22 installed next to a church in September 2010, a distinct slip surface was confirmed at around 15.4m depth, and the measurement has not been able to be implemented since November 2010 because of a deep bending of the pipe. It is considered, therefore, that there are slip surfaces around these depths accompanying active landslide movement.

At water level meter B27-09 (50m depth) installed on the roadside on June 2011, the steady water level of -15 to -16m had been recorded. However, the monitoring has never been implemented since July 26, 2011 because of the landslide movement. At water level meter B27-10 (25m depth) installed on the roadside on June 2011, the steady water level of -21 to -23m and the low water level of less than -25m at the end of July 2011 were recorded. At water level meter B27-21 (25m depth) installed on the roadside on September 2010, the steady water level of -22 to -23m and the high water level of -21.9m on September 29 in the rainy season were recorded. The steady water level keeps about -23 to -24m in the dry season. At water level meter B27-23 (25m depth) installed on the roadside in September 2010, the steady water level of -20 to -21m and the high water level of -20.3m on November 8 were recorded. However, there is no data after November 24 because the equipment was stolen.

#### e. Location L/S 28

At extensometer EX-6 installed on the step of the head of the landslide, extension movement started in early July and was continuously occurring until late November 2010, and the extension movement reached 211.8mm. The movement re-started on January 2011, and it reached 294.9mm in the end of June. It is considered, therefore, that the landslide intensively activates in the rainy season and is continuously moving even in the dry season.

At borehole extensometer B28-41 installed on the roadside in September 2010, there has been no movement even throughout the rainy season. It is considered, therefore, that there is no

landslide activity. Continued monitoring is required for confirmation.

At borehole inclinometer B28-11 installed on the roadside on September 2010, the measurement has not been able to be implemented since October 2010 because the bending of pipe occurred at around 14.7m depth. At borehole inclinometer B28-13 installed on the roadside in July 2011, the measurement has not been able to be implemented since the first measurement because the bending of pipe occurred at around 9.6m depth.

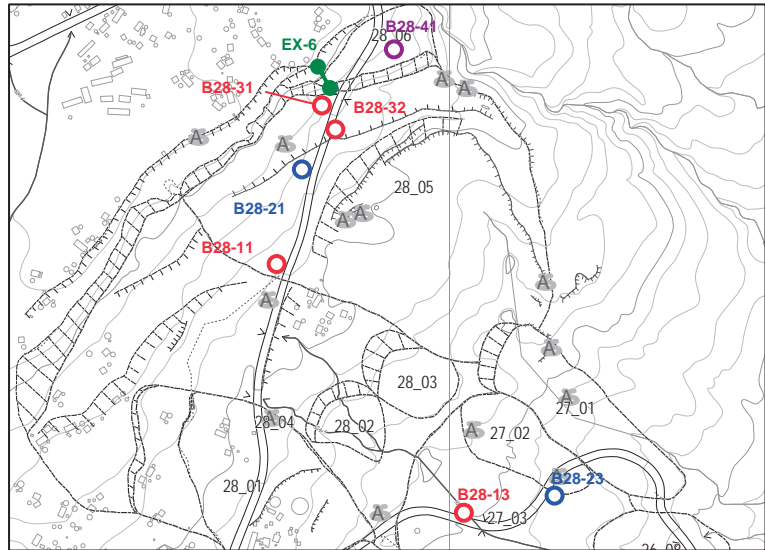


Figure 4.4.21 Location map of monitoring devices in L/S28

At borehole inclinometer B28-31 installed on the roadside in September 2010, a distinct slip surface was confirmed at around 14.0m depth, and the measurement has not been able to be implemented since December 2010 because of a deep bending of the pipe. At borehole inclinometer B28-32 installed on the roadside in October 2010, the measurement has not been able to be implemented since November 2010 because the bending of pipe occurred at around 24.5m depth. It is considered, therefore, that there are slip surfaces around these depths accompanying active landslide movement.

At water level meter B28-21 (25m depth) installed on the roadside in September 2010, both the steady water level and the high water level keeps around -20m. However, there is no data after November 24 because the equipment was stolen. At water level meter B28-23 (30m depth) installed on the roadside in June 2011, the rising up according to the rain and the high water level at -14.7m observed. The steady water level of -15 to -17m has been recorded after that.